ELSEVIER

Contents lists available at ScienceDirect

## Journal of Fluorine Chemistry

journal homepage: www.elsevier.com/locate/fluor



# Fluorinated Azaacenes: Efficient Syntheses, Structures, and Electrochemical Properties

Marc Zeplichal<sup>a</sup>, Joshua Gies<sup>a</sup>, Johannes Bernd<sup>a</sup>, Dilan Kancious Winslaws<sup>a</sup>, Tieyan Chang<sup>c</sup>, Yu-Sheng Chen<sup>c</sup>, Steven H. Strauss<sup>b,\*</sup>, Olga V. Boltalina<sup>b,\*</sup>, Andreas Terfort<sup>a,\*</sup>

- <sup>a</sup> Institut für Anorganische und Analytische Chemie, Goethe-Universität Frankfurt, 60438 Frankfurt am Main, Germany
- <sup>b</sup> Department of Chemistry, Colorado State University, Fort Collins, CO 80525, USA
- <sup>c</sup> ChemMatCARS, University of Chicago, Advanced Photon Source, Argonne, IL 60439, USA

#### ABSTRACT

Perfluoroalkylation is an effective strategy for lowering the valence orbital energies of arenes and is therefore used for the design of new n-type semiconductors. Here we present a strategy for the efficient reaction of the diazaarene phenazine (PHNZ) with 1,4-C<sub>4</sub>F<sub>8</sub>I<sub>2</sub>, which finally leads to the cyclization products 1,2- and 2,3-PHNZ (c-C<sub>4</sub>F<sub>8</sub>) (c- = cyclo-substituent). It turns out that the synthesis of these compounds can be attained with equal efficiacy by thermal reactions (in the presence of copper) or photochemical reactions (in the presence of photocatalysts, PC). While under the photochemical conditions, the reaction either stops after formation of a 1:1 mixture of cyclo-products with the mono-substituted compounds 1- and 2-PHNZ(c-C<sub>4</sub>F<sub>8</sub>I) (c- = c-tain with terminal substitution, PC: Ru(bpy)<sub>3</sub>Cl<sub>2</sub>) or even becomes reverted (PC: Rose Bengal), the thermal reaction is limited by the formation of the reduction products 1- and 2-PHNZ(c-C<sub>4</sub>F<sub>8</sub>H). Attempts to cyclize 1- and 2-PHNZ(c-C<sub>4</sub>F<sub>8</sub>I) thermally led to a new cyclic compound, 5-H-1,10-PHNZ(c-C<sub>3</sub>F<sub>6</sub>C(=O)), a cyclic amide derivative of 5,10-dihydrophenazine. Nevertheless, under photochemical conditions, the purified 1- and 2-PHNZ(c-C<sub>4</sub>F<sub>8</sub>I) could be cyclized cleanly to 1,2- and 2,3-PHNZ(c-C<sub>4</sub>F<sub>8</sub>). The cyclo-compounds could be reductively defluorinated under formation of a new aromatic ring, thus extending the  $\pi$ -systems to 1,2- and 2,3-PHNZ(c-C<sub>4</sub>F<sub>4</sub>), which are derivatives of benzo[a]phenazine and 5,12-diazaetracene, respectively. All these compounds could be isolated and were characterized by all or a subset of the following physicochemical techniques: a-1 and a-1 subset of the perfluoroalkyl groups could be verified, while the introduction of the (a-C<sub>4</sub>F<sub>4</sub>) annelation led to a significant lowering of the band gaps. The diazaeterracene derivative exposed a tendency for the [4+4] cyclodimerization to [2,3-PHNZ(a-C<sub>4</sub>F<sub>4</sub>)]<sub>2</sub>, which was also isolated and structurally characterized.

#### 1. Introduction

The fluorination, polyfluoroalkylation, and perfluoroalkylation of aromatic compounds is a vibrant field of synthetic fluorine chemistry driven by the needs of the pharmaceutical, agrochemical, and organic electronic industries [1–10]. The aromatic compounds that have been the focus of our research since 2013 are polycyclic aromatic hydrocarbons (PAHs), including those with one or more N atoms in their aromatic cores (azaPAHs) [11–19]. The preparation of most fluorinated/fluoroalkylated PAHs and azaPAHs typically involves multi-step "bottom-up" syntheses starting with *monocyclic* aromatic substrates containing fluorinated functional groups. A typical example is the five-step reaction sequence for the synthesis of hexabenzocoronene with polyfluoroalkyl chains [20]. Several examples of fluorinated and perfluoroalkylated azaPAH derivatives made by the bottom-up approach

are compounds A-D in Fig. 1 [21-26].

In contrast, direct attachments of  $C_xF_y$  substituents onto PAHs, aza-PAHs, or their halogenated derivatives are relatively rare. It has been demonstrated that aromatic ketones can be converted to perfluoroalkylated systems by the treatment with the Ruppert-Prakash reagent  $CF_3SiMe_3$  and its higher homologues, e.g. in the three-step sequence of reactions for the conversion of 6,13-pentacenequinone to 6,13-pentacene( $R_F$ )<sub>2</sub> derivatives ( $R_F$  = per- or polyfluoroalkyl chain) [24,27]. Sun and coworkers used perfluoroalkyl iodides ( $R_F$ I) to substitute Br atoms by  $R_F$  groups in the respective anthracene (ANTH), pyrene (PYRN), 1,10-phenanthroline, and dibenzo[a,c]phenazine derivatives by copper-mediated cross-coupling reactions [28,29]. Analogously, Chen and coworkers introduced a single  $\omega$ - $C_4F_8CI$  group to phenanthrene (PHAN) by heating 1,4- $C_4F_8CI$ , 9-iodo-PHAN, and Cu powder in DMSO at 80 °C [30]. Vicic and coworkers added a single

<sup>\*</sup> Corresponding author

Fig. 1. Highly fluorinated phenazines and related compounds reported in the literature before this work: A, ref. [21].; B, ref. [22].; C and D, ref. [23].; E-H, ref. [24].; I-L, ref. [14].; M-P, ref. [24].; Q, ref. [26]..

ω-C<sub>4</sub>F<sub>8</sub>Br group to 7-Cl-quinoline and naphthalene by heating the corresponding iodo compounds, CuI, and (1,10-phenanthroline)Ag (ω-C<sub>4</sub>F<sub>8</sub>Br) in acetonitrile at 50 °C (similarly, these authors also developed an elegant approach for the synthesis of arene(c-C<sub>4</sub>F<sub>8</sub>) derivatives by reaction of o-diiodoarenes (e.g. 2,3-diiodopyridine) with the organometallic complex (CH<sub>3</sub>CN)<sub>2</sub>Zn(1,4-C<sub>4</sub>F<sub>8</sub>)<sub>2</sub>Zn(NCCH<sub>3</sub>)<sub>2</sub> in DMF at 100 °C) [31-33]. Direct exchange reactions of H atoms at arenes have also been reported, e.g. by Qu, Wang, and coworkers, who introduced a single n-C $_8$ F $_{17}$  group into the unsubstituted PAHs PYRN and perylene (PERY) by reacting them with n-C<sub>8</sub>F<sub>17</sub>I and Cu powder in DMSO at 120 °C [34]. San and coworkers introduced a single perfluorobenzyl group (Bn<sub>F</sub>) to unsubstituted corannulene (CORA) by heating it with Bn<sub>F</sub>I and Cu powder in DMSO at 160 °C [18]. Pibiri and coworkers prepared PYRN(R<sub>F</sub>) derivatives photochemically by irradiating solutions of R<sub>F</sub>I and PYRN in CH<sub>3</sub>OH [35], and Iizuka and Yoshida prepared 1-naphthalene(n-C<sub>6</sub>F<sub>13</sub>) photochemically in CH<sub>3</sub>CN in the presence of TiO<sub>2</sub> as a photocatalyst [36]. Ono, Hisaeda, and coworkers prepared arene derivatives with annelated cyclo-C<sub>4</sub>F<sub>8</sub> substituents (hereinafter c-C<sub>4</sub>F<sub>8</sub>, such as e.g., 1-methylindole-2,3-c-C<sub>4</sub>F<sub>8</sub>) electrochemically using 1, 4-C<sub>4</sub>F<sub>8</sub>I<sub>2</sub> (hereinafter C<sub>4</sub>F<sub>8</sub>I<sub>2</sub>) in the presence of a catalytic amount of a vitamin  $B_{12}$  derivative [37].

We previously developed a direct method for the perfluoroalkylation of unsubstituted PAHs and azaPAHs in the gas phase that afforded libraries of PAH( $C_xF_y$ ) $_n$  and azaPAH( $C_xF_y$ ) $_n$  derivatives with strong electron acceptor properties [11–19]. When  $C_4F_8I_2$  was used as the  $C_xF_y$  reagent in high-temperature reactions with CORA, intranolecular cyclization to produce c- $C_4F_8$  derivatives was observed [12,16,17]. The CORA(c- $C_4F_8$ ) $_n$  derivatives with six- and seven-membered rings containing  $C_4F_8$  moieties were found to have gas-phase electron affinities (EAs) up to 2.3 eV higher than the 0.5 eV EA of unsubstituted CORA [12]. One compound, CORA(c- $C_4F_8$ ) $_3$ , is a stronger electron acceptor

than the fullerene  $C_{60}$  [12]. Reactions of  $C_4F_8I_2$  with triphenylene (TRPH) at 300 °C also afforded derivatives with up to three  $c\text{-}C_4F_8$  substituents [16,17]. When the reactions were performed at 360 °C in the presence of activated Cu powder, reductive defluorination/aromatization (RDF/A) of one or more of the aliphatic six-membered rings with  $C_4F_8$  moieties to aromatic six-membered rings with  $C_4F_8$  moieties was observed [16,17]. Although the yield and selectivity were low in this case [17], the conversion of  $c\text{-}C_4F_8$  substituents to  $c\text{-}C_4F_4$  substituents by RDF/A, in general, would be a valuable and convenient method to expand the aromatic core of a PAH with fluorinated aromatic rings if yields and selectivities could be improved.

Examples of PHNZ derivatives with  $CF_3$ , c- $C_4F_8$ , and c- $C_4F_4$  substituents, which we prepared in previous work by gas-phase high-temperature reactions, are compounds E-L in Fig. 1 [14,24]. In this work, several new methods with significantly milder reaction conditions were developed for the substitution of c- $C_4F_8$  groups onto PHNZ. These include moderate heating of reaction mixtures in suitable organic solvents as well as room-temperature photochemical reactions. In addition, we report the RDF/A of PHNZ(c- $C_4F_8$ ) with Zn powder at 200 °C to quantitatively produce PHNZ(c- $C_4F_8$ ).

#### 2. Results and Discussion

#### 2.1. Synthesis

In this work, thermal and photochemical reactions of PHNZ with  $C_4F_8I_2$  in organic solvents were studied at temperatures ranging from 25 °C to 200 °C. The ten fluorinated phenazine derivatives obtained are shown in Fig. 2. First, we will discuss the results of the thermal reactions (Section 2.1.1.), followed by those obtained with photochemistry (Section 2.1.2.). In a third section, we will report on the cyclization reaction

Fig. 2. The fluorinated phenazines synthesized and characterized in this work. Their abbreviations are also shown. A drawing of unsubstituted phenazine (PHNZ) showing IUPAC locants is at the upper left.

of the  $\omega$ -C<sub>4</sub>F<sub>8</sub>I derivatives, before we discuss the reductive defluorination of the c-C<sub>4</sub>F<sub>8</sub> derivatives to the aromatic c-C<sub>4</sub>F<sub>4</sub> systems (Section 2.1.4.). In Section 2.1.5., finally some alternative approaches and their results will be presented. In these sections, reaction conditions and yields are discussed, while additional details can be found in the ESI.

#### 2.1.1. Thermal reactions in Organic Solvents

2.1.1.1. Background. Previous work by Boltalina and coworkers, which yielded dozens of new PAH(R<sub>F</sub>)<sub>n</sub> and azaPAH(R<sub>F</sub>)<sub>n</sub> compounds, involved heating the unsubstituted PAH or azaPAH with gaseous R<sub>F</sub>I reagents in sealed glass ampoules or corrosion-resistant autoclaves at 300–360 °C [11–19]. The elevated temperatures caused homolytic C–I bond cleavage, attachment of the R<sub>F</sub>• radical to the substrate, and removal of an H atom by a second R<sub>F</sub>• radical. In one reaction with CF<sub>3</sub>I, CHF<sub>3</sub> was identified as one of the products along with I<sub>2</sub> and the PAH(CF<sub>3</sub>)<sub>n</sub> derivatives [13]. Interestingly, the attack of a R<sub>F</sub>• radical at one of the  $\beta$  positions of tetraarylporphyrins was not followed by H atom abstraction, and perfluoroalkyl chlorins [i.e., perfluoroalkyl dihydroporphyrins] were isolated [38]. In some of the high-temperature reactions, Cu powder was added to the reaction mixture to promote C–I bond cleavage (presumably with concomitant CuI formation).

The goal of the previous work was to prepare and characterize as many isomers with the general composition of  $PAH(R_F)_n$  as possible in order to study differences in their electronic properties as a function of n and isomer structure, rather than to prepare any particular product with high selectivity. Nevertheless, in some cases particular compounds were preferentially formed and could be isolated in yields up to 60% [13,17]. However, many organic substrates cannot withstand such high temperatures, and lower temperature reactions of PAHs, R<sub>F</sub>I reagents, and Cu powder in an organic solvent have been used with some success in the past. For instance, the compound 9-PHAN(ω-C<sub>4</sub>F<sub>8</sub>Cl) was prepared in 53% yield in DMSO at 80 °C [30]. Similarly, the compounds 1-PERY  $(C_8F_{17})$  and 1-PYRN $(C_8F_{17})$  could be obtained in 65% and 70% yield, respectively, in DMSO at 120 °C [34]. The compound 1-CORA(Bn<sub>E</sub>) was prepared in 29% yield in DMSO at 160 °C [18]. However, there was no reaction between bromopentacenes, RFI, and Cu powder in DMSO at 110 °C [39].

2.1.1.2. Results obtained by Thermal Reactions. The reaction of PHNZ,  $C_4F_8I_2$ , and activated Cu powder in 1,2-dichlorobenzene (DCB) has been reported before [14,24]. In our hands, this reaction either at 120 °C or 160 °C resulted only in minor amounts ( $\leq$  2%) of the desired products 1- and 2-PHNZ( $\omega$ - $C_4F_8I$ ) (these two compounds are hereinafter

**Table 1**Experimental conditions and products of anaerobic thermal reactions of PHNZ with C4F8I2 and Cu powder in organic solvents. a,b

	conditions			reagents			products		
rxn.	solvent	time, h	temp., °C	PHNZ, mmol (mg)	1,4-C <sub>4</sub> F <sub>8</sub> I <sub>2</sub> , mmol (equiv.)	Cu powder, mmol (equiv.)	major products (% by GCMS) <sup>c</sup>	minor products ( $\leq 2\%$ by GCMS) <sup>c</sup>	
T1	DCB	6	160	0.277 (50.0)	1.1 (4.0)	15.3 (55.2)	3-DCB( $\omega$ -C <sub>4</sub> F <sub>8</sub> I) (8), 4-DCB( $\omega$ -C <sub>4</sub> F <sub>8</sub> I) (83)	PHNZ( $C_4F_8$ ), PHNZ( $C_4F_8I$ ), PHNZ( $C_4F_{4-x}H_x$ )	
T2	DCB	12	120	0.277 (50.0)	1.1 (4.0)	15.2 (54.9)	$3-DCB(\omega-C_4F_8I)$ (8), $4-DCB(\omega-C_4F_8I)$ (83)	PHNZ( $C_4F_8$ ), PHNZ( $C_4F_8I$ ), PHNZ( $C_4F_{4-x}H_x$ )	
Т3	TCB	6	160	0.277 (50.0)	1.1 (4.0)	15.0 (54.2)	no major products	PHNZ( $c$ -C <sub>4</sub> F <sub>8</sub> ), PHNZ ( $\omega$ -C <sub>4</sub> F <sub>8</sub> I)	
T4	HFB <sup>d</sup>	6	110	0.0832 (15.0)	0.33 (4.0)	4.70 (56,5)	no major products	PHNZ( <i>c</i> -C <sub>4</sub> F <sub>8</sub> ), PHNZ( <i>c</i> -C <sub>4</sub> F <sub>8</sub> ) <sub>2</sub>	
T5	MES	6	160	0.282 (50.8)	1.13 (4.0)	16.0 (56.7)	none (no reaction)	none (no reaction)	
Т6	DMSO	12	120	0.277 (50.0)	1.1 (4.0)	11.8 (42.6)	no major products	PHNZ( $c$ -C <sub>4</sub> F <sub>8</sub> ), PHNZ ( $\omega$ -C <sub>4</sub> F <sub>8</sub> H)	
T7	DMF	6	160	0.277 (50.0)	1.1 (4.0)	15.3 (55.2)	PHNZ( $c$ -C <sub>4</sub> F <sub>8</sub> ) (18), PHNZ( $\omega$ -C <sub>4</sub> F <sub>8</sub> H) (22)	PHNZ( $\omega$ -C <sub>4</sub> F <sub>8</sub> I)	
T8	DMF	8	160	0.277 (50.0)	1.1 (4.0)	15.2 (54.9)	PHNZ( $c$ -C <sub>4</sub> F <sub>8</sub> ) (32), PHNZ( $\omega$ -C <sub>4</sub> F <sub>8</sub> H) (35)	PHNZ( $\omega$ -C <sub>4</sub> F <sub>8</sub> I)	
T9	DMF	10	160	0.277 (50.0)	1.1 (4.0)	15.0 (54.2)	PHNZ( $c$ -C <sub>4</sub> F <sub>8</sub> ) (45), PHNZ( $\omega$ -C <sub>4</sub> F <sub>8</sub> H) (50)	PHNZ( $\omega$ -C <sub>4</sub> F <sub>8</sub> I)	
T10	DMF	12	160	0.277 (50.0)	1.1 (4.0)	15.0 (54.2)	PHNZ( $c$ -C <sub>4</sub> F <sub>8</sub> ) (45), PHNZ( $\omega$ -C <sub>4</sub> F <sub>8</sub> H) (50)	PHNZ( $\omega$ -C <sub>4</sub> F <sub>8</sub> I)	
T11	DMF <sup>e</sup>	0.3	200	0.0832 (15.0)	0.090 (1.1)	none	PHNZ( <i>c</i> -C <sub>4</sub> F <sub>8</sub> ) (28), PHNZ( <i>ω</i> -C <sub>4</sub> F <sub>8</sub> H) (18), 5- H-1,10-PHNZ( <i>c</i> -C <sub>3</sub> F <sub>6</sub> C(=O)) (23)	none observed	
T12	DMA	6	160	0.280 (50.5)	0.31 (1.1)	16.2 (57.9)	PHNZ( $c$ -C <sub>4</sub> F <sub>8</sub> ) (12), PHNZ( $\omega$ -C <sub>4</sub> F <sub>8</sub> H) (9)	5-H-1,10-PHNZ( <i>c</i> -C <sub>3</sub> F <sub>6</sub> C (=O))	
T13	TFDMA	6	160	0.280 (50.5)	0.31 (1.1)	15.7 (56.1)	PHNZ( $c$ -C <sub>4</sub> F <sub>8</sub> ) (18), PHNZ( $\omega$ -C <sub>4</sub> F <sub>8</sub> I) (11)	none observed	

<sup>a</sup>Abbreviations: PHNZ, phenazine; DCB, 1,2-dichlorobenzene; TCB, 1,2,4-trichlorobenzene; MES, mesitylene  $(1,3,5\text{-}C_6H_3(\text{CH}_3)_3)$ ; HFB, hexafluorobenzene; DMSO, dimethyl-sulfoxide; DMF, *N*,*N*-dimethylformamide; DMA, *N*,*N*-dimethylacetamide; TFDMA, 2,2,2-trifluoro-*N*,*N*-dimethylacetamide; PHNZ(c-C<sub>4</sub>F<sub>8</sub>), mixture of 1,2-and 2,3-PHNZ(c-C<sub>4</sub>F<sub>8</sub>). <sup>b</sup>Reactions were carried out in Schlenk flasks unless otherwise indicated. The reaction volume was 5.0 mL except reactions T4 (1.5 mL) and T11 (1.0 mL) <sup>c</sup> PHNZ( $\omega$ -C<sub>4</sub>F<sub>8</sub>I) and PHNZ( $\omega$ -C<sub>4</sub>F<sub>8</sub>H) products consisted of both 1- and 2- isomers. <sup>d</sup> This reaction was carried out in a sealed glass ampoule (see Supporting Information). <sup>e</sup> This reaction was carried out in a microwave reactor (see Supporting Information). The microwave power was adjusted, via feedback from a probe, to keep the reaction mixture from exceeding 200 °C.

collectively referred to as PHNZ(\omega-C\_4F\_8I)), and 1,2- and 2,3-PHNZ (c-C<sub>4</sub>F<sub>8</sub>) (hereinafter collectively referred to as PHNZ(c-C<sub>4</sub>F<sub>8</sub>)). Instead, the main reaction products were identified as 3- and 4-DCB( $\omega$ -C<sub>4</sub>F<sub>8</sub>I) in a total yield of 90% yield based on C<sub>4</sub>F<sub>8</sub>I<sub>2</sub>. As 4-DCB( $\omega$ -C<sub>4</sub>F<sub>8</sub>I) is reported here for the first time, its characterization is detailed in the ESI. To suppress the participation of the solvent in the reaction, alternatively 1,2,4-trichlorobenzene (TCB), hexafluorobenzene (HFB), mesitylene (MES), N,N-dimethylacetamide (DMA), 2,2,2-trifluoro-N,N-dimethylacetamide (TFDMA), DMSO, and DMF were employed at reaction temperatures of 110-160 °C (benzene and xylenes were not used, because they had previously been shown to undergo perfluoroalkylation [40,41], processes that would also compete with the perfluoroalkylation of PHNZ). The results are listed in Table 1 (more details are given in Tables S1 and S2 and the experimental part in the ESI). None of the three alternative aromatic solvents gave acceptable results. The reaction in DMSO at 120 °C also produced only minor amounts of the desired products, even after 12 h. This is in contrast to the reported preparation of 1-PERY(C<sub>8</sub>F<sub>17</sub>) and 1-PYRN(C<sub>8</sub>F<sub>17</sub>) in satisfactorily yields in DMSO at 120 °C [34].

Reactions in DMF at 160 °C produced a mixture of 1,2-PHNZ(c-C<sub>4</sub>F<sub>8</sub>) and 2,3-PHNZ(c-C<sub>4</sub>F<sub>8</sub>) in up to 45% yield based on PHNZ. The yield increased as a function of reaction time, from 18% after 6 h, to 32% after 8 h, to 45% after 10 h, but stayed at this level at 12 h. Only minor amounts of 1-PHNZ( $\omega$ -C<sub>4</sub>F<sub>8</sub>I) and 2-PHNZ( $\omega$ -C<sub>4</sub>F<sub>8</sub>I) were observed. However, the compounds 1-PHNZ( $\omega$ -C<sub>4</sub>F<sub>8</sub>H) and 2-PHNZ( $\omega$ -C<sub>4</sub>F<sub>8</sub>H), which cannot undergo ring closure, were formed in amounts equal to or exceeding the ones of the PHNZ(c-C<sub>4</sub>F<sub>8</sub>) isomers. Since the combined yields of the PHNZ(c-C<sub>4</sub>F<sub>8</sub>) and PHNZ( $\omega$ -C<sub>4</sub>F<sub>8</sub>H) derivatives are 95% after 10 or 12 h, the H atoms in the latter products cannot originate from unreacted PHNZ, but rather from the solvent, DMF, or products of its degradation. It has been reported that other aromatic compounds with  $\omega$ -C<sub>4</sub>F<sub>8</sub>H substituents have been produced in reactions with 1,4-C<sub>4</sub>F<sub>8</sub>Br<sub>2</sub> as well as with C<sub>4</sub>F<sub>8</sub>I<sub>2</sub> [37].

Similar reactions were also carried out in DMA. Only 1.1 equiv. of  $C_4F_8I_2$  was used as compared to 4.0 equiv. in the DMF reactions. After 6 h at 160 °C, the yield of PHNZ(c- $C_4F_8$ ) was 12% (cf. 18% in DMF) and the yield of PHNZ( $\omega$ - $C_4F_8$ H) was 9% (cf. 22% in DMF). Using TFDMA

under the same conditions, the products obtained after 6 h (reaction T13 in Table 1) differed significantly from the ones obtained in DMF and DMA. While the amount of PHNZ(c-C<sub>4</sub>F<sub>8</sub>) was similar to the one formed in DMF (18%), the PHNZ( $\omega$ -C<sub>4</sub>F<sub>8</sub>I) isomers were also major products (with a combined yield of 11% yield), and no PHNZ( $\omega$ -C<sub>4</sub>F<sub>8</sub>H) were found. From this observation, we deduce that the H atom abstraction from the CH<sub>3</sub> groups on the N atoms in DMF, DMA, and TFDMA is much slower than H atom abstraction from the CHO and the CH<sub>3</sub>CO group in DMF and DMA, respectively, what might be explained by the literature-known effect that the abstraction of H atoms does not only depend on the C-H bond energy, but also on the nature of the attacking radical as well (in the condensed phase) and on solvent polarity [42,43].

A reaction in DMF without Cu powder was carried out using microwave radiation. After heating the reaction mixture to 200 °C for 18 min (Reaction T11 in Table 1), three major products, PHNZ(c-C<sub>4</sub>F<sub>8</sub>) (28%), PHNZ( $\omega$ -C<sub>4</sub>F<sub>8</sub>H) (18%), and 5-H-1,10-PHNZ(c-C<sub>3</sub>F<sub>6</sub>C(=O)) (23%), were produced. The latter compound, shown in Fig. 2, is reported for the first time. Whether the oxygen atom in the molecules stems from the solvent, its decomposition products or adventitious water is not clear at this time. This compound is formally a tricyclic amide derivative of 5,10-dihydrophenazine, with the carbonyl C atom attached to the proximate N atom. The structure of this unusual product, determined by single-crystal X-ray diffraction, will be discussed below, in Section 3.

## 2.1.2. Photochemical Reactions in Organic Solvents

2.1.2.1. Background. Photochemical perfluoroalkylation of organic substrates has been actively developed as an alternative to thermal reactions [3,35,36,44–48]. Several examples relevant to this work, the photochemical preparation of PYRN(R<sub>F</sub>) [35] and naphthalene(R<sub>F</sub>) [36], were already mentioned in the Introduction. In a reaction, that is particularly relevant to this work, Postigo and coworkers used C<sub>4</sub>F<sub>8</sub>I<sub>2</sub> to introduce an  $\omega$ -C<sub>4</sub>F<sub>8</sub>I group to aniline photochemically in CH<sub>3</sub>CN in the presence of Cs<sub>2</sub>CO<sub>3</sub> as a base and Rose Bengal as a non-metal photocatalyst (PC) [46]. Significantly, the 65% yield mixture of *ortho*- and *para*-aniline( $\omega$ -C<sub>4</sub>F<sub>8</sub>I) did not undergo cyclization to aniline(c-C<sub>4</sub>F<sub>8</sub>) under the photochemical reaction conditions [46].

**Table 2**Experimental conditions and products of batch photo-reactions in dry acetonitrile. <sup>a</sup>

rxn.	condit time	ions vol.,	PHNZ, mmol	reagents 1,4-C <sub>4</sub> F <sub>8</sub> I <sub>2</sub> , mmol	PC, µmol	base, mmol	products major constituents of product mixture	minor products ( $\leq$ 2% by
		mL	(mg)	(equiv)	(equiv.) <sup>b</sup>	(equiv.) <sup>c</sup>	(% by GCMS) <sup>d</sup>	GCMS) <sup>e</sup>
P1A <sup>f</sup>	18 h	3.0	0.600 (108)	1.8 (3.0)	none	0.9 (1.5)	PHNZ (89), PHNZ( $\omega$ -C <sub>4</sub> F <sub>8</sub> I) (10)	PHNZ(c-C <sub>4</sub> F <sub>8</sub> )
P1B <sup>f</sup>	15 d	3.0	0.600 (108)	1.8 (3.0)	none	0.9 (1.5)	PHNZ (49), PHNZ( $\omega$ -C <sub>4</sub> F <sub>8</sub> I) (23), PHNZ ( $c$ -C <sub>4</sub> F <sub>8</sub> ) (27)	PHNZ(R <sub>F</sub> ) <sub>2</sub>
P2 <sup>f</sup>	7 d	1.5	0.277 (50.0)	1.6 (6.0)	14 (0.05)	0.8 (3)	PHNZ (50); PHNZ( $\omega$ -C <sub>4</sub> F <sub>8</sub> I) (27), PHNZ ( $c$ -C <sub>4</sub> F <sub>8</sub> ) (23)	PHNZ(c-C <sub>4</sub> F <sub>8</sub> )
P3 <sup>g</sup>	48 h	2.5	0.544 (100)	0.555 (1.0)	28 (0.05)	0.83 (1.5)	PHNZ (50), PHNZ( $\omega$ -C <sub>4</sub> F <sub>8</sub> I) (25), PHNZ ( $c$ -C <sub>4</sub> F <sub>8</sub> ) (25)	PHNZ(R <sub>F</sub> ) <sub>2</sub>
P4A <sup>h</sup>	12 h	2.5	0.544 (100)	0.555 (1.0)	28 (0.05)	0.83 (1.5)	PHNZ (2); PHNZ( $\omega$ -C <sub>4</sub> F <sub>8</sub> I) (70), PHNZ ( $c$ -C <sub>4</sub> F <sub>8</sub> ) (28)	PHNZ(R <sub>F</sub> ) <sub>2</sub>
4B <sup>h</sup>	24 h	2.5	0.544 (100)	0.555 (1.0)	28 (0.05)	0.83 (1.5)	PHNZ (2), PHNZ( $\omega$ -C <sub>4</sub> F <sub>8</sub> I) (49), PHNZ ( $c$ -C <sub>4</sub> F <sub>8</sub> ) (49)	PHNZ(R <sub>F</sub> ) <sub>2</sub>
P4C <sup>h</sup>	36 h	2.5	0.544 (100)	0.555 (1.0)	28 (0.05)	0.83 (1.5)	PHNZ (12); PHNZ( $\omega$ -C <sub>4</sub> F <sub>8</sub> I) (44), PHNZ ( $c$ -C <sub>4</sub> F <sub>8</sub> ) (44)	PHNZ(R <sub>F</sub> ) <sub>2</sub>
P4D <sup>h</sup>	48 h	2.5	0.544 (100)	0.555 (1.0)	28 (0.05)	0.83 (1.5)	PHNZ (35), PHNZ(ω-C <sub>4</sub> F <sub>8</sub> I) (32), PHNZ (c-C <sub>4</sub> F <sub>8</sub> ) (32)	PHNZ(R <sub>F</sub> ) <sub>2</sub>
P4E <sup>h</sup>	72 h	2.5	0.544 (100)	0.555 (1.0)	28 (0.05)	0.83 (1.5)	PHNZ (100)	none
P5 <sup>i</sup>	12 h	4.5	0.280 (50.5)	0.28 (1.0)	2.8 (0.01)	0.84 (3)	PHNZ (5); PHNZ( $\omega$ -C <sub>4</sub> F <sub>8</sub> I) (45), PHNZ ( $c$ -C <sub>4</sub> F <sub>8</sub> ) (50)	PHNZ(\omega-C_4F_8H)

a The reactions were run at ambient temperature with the light source water- or air cooled unless otherwise indicated. Abbreviations: PHNZ, phenazine; PC, photocatalyst added to the reaction mixture; PHNZ(c-C<sub>4</sub>F<sub>8</sub>), a mixture of 1,2- and 2,3-PHNZ(c-C<sub>4</sub>F<sub>8</sub>). There was no PC used for reactions P1A and P1B. The PC used for reactions P2, P3, and P4A–E was the disodium salt of Rose Bengal. The PC used for reaction P5 was Ru(bpy)<sub>3</sub>Cl<sub>2</sub>. The base used was Cs<sub>2</sub>CO<sub>3</sub> except for reaction P5, in which the base used was tetramethylethylenediamine. PHNZ( $\omega$ -C<sub>4</sub>F<sub>8</sub>I) products consisted of a mixture of 1-PHNZ( $\omega$ -C<sub>4</sub>F<sub>8</sub>I) and 2-PHNZ( $\omega$ -C<sub>4</sub>F<sub>8</sub>I). R<sub>F</sub> = c-C<sub>4</sub>F<sub>8</sub> and/or  $\omega$ -C<sub>4</sub>F<sub>8</sub>I and/or  $\omega$ -C<sub>4</sub>F<sub>8</sub>H. See ESI for details about which minor products were present. The light source was a 25 W water-cooled medium pressure mercury vapor lamp. The light source was a pair of 40 W LEDs; the reaction mixture was not water-cooled, i.e. it was not at ambient temperature. The light source was a pair of 20 W LEDs; the reaction mixture was water-cooled.

2.1.2.2. Batch Photochemical Reactions with PHNZ. Photochemical reactions of PHNZ with  $C_4F_8I_2$  were studied with the goal of preparing cyclic derivatives in a scalable single-step process and with larger yields than obtained in thermal reactions in solution or in the gas phase. The results are listed in Table 2.

A mixture of PHNZ, 3 equiv. C<sub>4</sub>F<sub>8</sub>I<sub>2</sub>, and 1.5 equiv. Cs<sub>2</sub>CO<sub>3</sub> in dry CH<sub>3</sub>CN was irradiated at room-temperature with a water-cooled 25 W medium pressure Hg vapor lamp in the absence of a PC, initially for 18 h (Reaction P1A, see set-up in Fig. S1 in the ESI). The major constituents of the product mixture were unreacted PHNZ (89% by GCMS) and the two isomers of PHNZ(\omega-C\_4F\_8I) (10\% by GCMS). A small amount (less than 2%) of PHNZ(c-C<sub>4</sub>F<sub>8</sub>) was also present, showing that cyclization of the ω-C<sub>4</sub>F<sub>8</sub>I substituent can occur under photochemical conditions. After 15 days, more PHNZ was converted to these products, and the PHNZ (ω-C<sub>4</sub>F<sub>8</sub>I) isomers underwent cyclization (Reaction P1B). The mixture of major constituents contained 49% PHNZ, 23% PHNZ(\omega-C\_4F\_8I), and 27% PHNZ(*c*-C<sub>4</sub>F<sub>8</sub>). When the reaction was performed in the presence of 0.05 equiv. Rose Bengal as PC, the same mixture of major constituents, with comparable yields, was also present after only 7 days (Reaction P2). The use of Rose Bengal as PC opened the opportunity to use light of longer wavelength for the photoreaction, such as the white light emitted by a light-emitting diode (LED, typically 420 - 700 nm, see Figures S2 and S3 in ESI). When the reaction mixture was irradiated for 48 h with two LEDs (each run at 40 W), without cooling the reaction mixture, the same mixture of major constituents in comparable yields as with the Hg vapor lamp was obtained (Reaction P3; see Figure S4 in the ESI for the experimental arrangement of sample vial and LEDs). The fact that aniline(ω-C<sub>4</sub>F<sub>8</sub>I) did not undergo photolytic cyclization to aniline(c-C<sub>4</sub>F<sub>8</sub>) in ref. [46]. might be explained by the use of a weaker light source, a 60 W fluorescent light bulb, along with a shorter reaction time of 24 h.

The reason that PHNZ is listed as "a major constituent of the product mixture" instead of "unreacted PHNZ in the product mixture" in Table 2 is because it was found that prolonged irradiation in the presence of Rose Bengal converted both, PHNZ(c-C<sub>4</sub>F<sub>8</sub>) and PHNZ( $\omega$ -C<sub>4</sub>F<sub>8</sub>I), back to unsubstituted PHNZ (Reactions P4A–P4E). E.g., after 12 h, only 2% PHNZ was left and 70% PHNZ( $\omega$ -C<sub>4</sub>F<sub>8</sub>I) and 28% of the cyclization product PHNZ(c-C<sub>4</sub>F<sub>8</sub>) had formed. The same amount of PHNZ was

present, and more PHNZ( $\omega$ -C<sub>4</sub>F<sub>8</sub>I) had undergone cyclization to PHNZ (c-C<sub>4</sub>F<sub>8</sub>) (both were present at 49%), after 24 h. However, upon continued irradiation more and more PHNZ reformed in the product mixture amounting to 12% after 36 h, 35% after 48 h, and 100% after 72 h. There was a concomitant photobleaching of Rose Bengal observed during the 72 h photolysis reaction. Oxidative as well as reductive photobleaching of Rose Bengal is well documented [49], and could be related to the back-conversion of PHNZ( $\omega$ -C<sub>4</sub>F<sub>8</sub>I) and PHNZ(c-C<sub>4</sub>F<sub>8</sub>) to PHNZ( $\varepsilon$ -C<sub>4</sub>F<sub>8</sub>I)

To address the problem with photobleaching, an alternative PC, Ru(bpy) $_3$ Cl $_2$ , was employed together with tetramethylethylenediamine (TMEDA) as the base (instead of Cs $_2$ CO $_3$ ) in Reaction P5. This was a 12 h reaction running the two LEDs at 20 W, which produced 50% PHNZ (c-C $_4$ F $_8$ ) and 45% PHNZ( $\omega$ -C $_4$ F $_8$ I), with only 5% PHNZ in the product mixture. As the color of the reaction mixture did not change visibly, we assume that no (or only minor) photobleaching of Ru(bpy) $_3^{2+}$  occured. These were the best photochemical conditions for a batch reaction in this study, so we adopted them to the flow reaction conditions described in the next paragraph as soon as we found them.

2.1.2.3. Flow Photochemical Reactions with PHNZ. In our search for a scalable photochemical method, we decided to use flow photochemistry, which had been developed during the past decade as a more efficient and economical photochemical methodology [50]. Furthermore, successful continuous-flow photochemical perfluoroalkylations of small organic substrates have been reported [51,52].

ESI Figures S5 and S6 show the capillary-flow device constructed for single flow reactions. The capillary was 1/8 in. FEP tubing coiled around a water-cooled aluminum heat exchanger, the construction plan of which is shown in ESI Figure S7. A syringe pump was used to flow the reaction mixture past two variable-intensity (100 W maximum power) LED chips. There was no heating of the reaction mixture using this setup.

Initial reactions were performed using Rose Bengal as the PC. However, due to the relatively low solubility of Rose Bengal and  $Cs_2CO_3$  in  $CH_3CN$ , sedimentation was observed in the syringe and in the capillary. Furthermore, photobleaching of Rose Bengal took place over time,

which lowered the PC concentration and had a detrimental effect on PHNZ conversion to the desired products. The effect of Rose Bengal photobleaching was minimized by using a recirculating photochemical apparatus with a peristaltic pump, which is shown in ESI Figures S8 and S9. The flow rate was 1 mL min $^{-1}$  with an 8 min residence time in the illuminated capillary. Rose Bengal was added sequentially over 18 h in five equal portions.

As the batch photochemical reaction P5 had shown that Ru(bpy)<sub>3</sub>Cl<sub>2</sub> was effective for PHNZ/C<sub>4</sub>F<sub>8</sub>I<sub>2</sub> reactions in CH<sub>3</sub>CN, we continued the experiments with this PC. The system has the additional advantage that the use of the base TMEDA, in contrast to Cs<sub>2</sub>CO<sub>3</sub>, avoided precipitation in the capillary. With this combination, reaction conditions using the recirculating photochemical apparatus were optimized, resulting in improved isolated yields of PHNZ(c-C<sub>4</sub>F<sub>8</sub>) and PHNZ(\omega-C<sub>4</sub>F<sub>8</sub>I) (45% each, i.e., 90% combined isolated yield based on PHNZ). The optimized reaction required less time for complete PHNZ conversion, the amount of PC could be lowered from 0.05 equiv. with Rose Bengal to 0.01 equiv. with Ru(bpy)<sub>3</sub>Cl<sub>2</sub>, and LED power of only 20 W per chip was needed as compared to 40 W per chip required for the Rose Bengal reactions. Unsubstituted PHNZ was easily removed from the product mixture by flash chromatography, which was followed by isolation of the pure perfluoroalkylphenazine derivatives using an automated flash chromatography system with a gradient of 25% CH<sub>2</sub>Cl<sub>2</sub> in n-hexane to 100% CH<sub>2</sub>Cl<sub>2</sub> (see the ESI chapter SII.3.2. for more details).

#### 2.1.3. Cyclization of 1-PHNZ( $\omega$ -C<sub>4</sub>F<sub>8</sub>I)

Efforts to optimize the photochemical reaction towards complete conversion of PHNZ to PHNZ( $c\text{-}C_4F_8$ ) were not successful. At best we were able to prepare a 50/50 mixture of PHNZ( $\omega\text{-}C_4F_8$ I) and PHNZ( $c\text{-}C_4F_8$ ) in a 24 h reaction with Rose Bengal or a 12 h reaction with Ru(bpy) $_3\text{Cl}_2$ . We thus investigated an alternative method to convert the PHNZ( $\omega\text{-}C_4F_8$ I) of the reaction mixture to PHNZ( $c\text{-}C_4F_8$ ) in a sequential step, i.e. thermal activation after the photochemical reaction. In a first experiment, a sample of the crude reaction mixture prepared in Reaction P4D was used, prior to the removal of Rose Bengal and the Cs salts. The sample in the sealed reaction vessel was placed in a microwave reactor and subjected to a short microwave treatment of 8 min at 160 °C. GCMS analysis showed that complete degradation of all PHNZ( $R_F$ ) $_n$  products originally present in the sample had occurred, all the way down to parent PHNZ ( $R_F$  is used here as an abbreviation for c-C<sub>4</sub>F<sub>8</sub> and/or  $\omega$ -C<sub>4</sub>F<sub>8</sub>II and/or  $\omega$ -C<sub>4</sub>F<sub>8</sub>II).

To determine whether rapid thermal degradation of PHNZ( $R_F$ )<sub>n</sub> would occur in the absence of Rose Bengal and base (i.e., whether PHNZ ( $R_F$ )<sub>n</sub> derivatives are intrinsically thermally stable or unstable), a purified sample of PHNZ(c- $C_4F_8$ ) was dissolved in dry CH<sub>3</sub>CN, placed in a sealed reaction vessel, and heated in the microwave reactor to 160 °C for

8 min. GCMS analysis showed that no thermal degradation of PHNZ(c- $C_4F_8$ ) had occurred, demonstrating that Rose Bengal, or its photobleaching products, caused the loss of  $R_F$  groups from PHNZ( $R_F$ ) $_n$  thermally (and undoubtedly is also responsible for the gradual degradation of PHNZ( $R_F$ ) $_n$  during photochemical reactions).

With this result at hand, we examined if the purified isomer 1-PHNZ  $(\omega$ -C<sub>4</sub>F<sub>8</sub>I) could be converted into 1,2-PHNZ(c-C<sub>4</sub>F<sub>8</sub>) thermally. When a sample of solid 1-PHNZ(ω-C<sub>4</sub>F<sub>8</sub>I) was sealed in a large glass ampoule and heated to 175 °C, the faint violet color in the ampoule indicated the formation of elemental I2, and hence successful cleavage of C-I bonds. The soluble fraction (roughly 50%) of the crude product was extracted from the ampoule and analyzed spectroscopically. Instead of the expected cyclic compound 1,2-PHNZ(c-C<sub>4</sub>F<sub>8</sub>), the new tricyclic amide derivative of 5,10-dihydrophenazine, 5-H-1,10-PHNZ(c-C<sub>3</sub>F<sub>6</sub>C(=O)), was formed. The insoluble part of the product in the ampoule had the appearance of polymerized products (possibly via intermolecular perfluoroalkylation) and was not analyzed further. When the same reaction was performed in dry CH<sub>3</sub>CN by microwave heating to 160 °C for 8 min, the conversion to 5-H-1,10-PHNZ(c-C<sub>3</sub>F<sub>6</sub>C(=O)) was even quantitative. It remains unclear, where the oxygen atom of the formal hydrolysis product originates from, and the participation of the glass container (by reaction with intermediately formed HF) cannot be excluded.

Finally, photoinduced cyclization was achieved by irradiating a mixture of purified 1-PHNZ( $\omega$ -C<sub>4</sub>F<sub>8</sub>I), Rose Bengal, and Cs<sub>2</sub>CO<sub>3</sub> in dry degassed CH<sub>3</sub>CN in the recirculating capillary flow reactor for 3 h. This reaction produced an 87% isolated yield of 1,2-PHNZ(c-C<sub>4</sub>F<sub>8</sub>I). Unreacted 1-PHNZ( $\omega$ -C<sub>4</sub>F<sub>8</sub>I) was also recovered. Notably, no formation of 5-H-1,10-PHNZ(c-C<sub>3</sub>F<sub>6</sub>C(=O)) was observed, even in a trace amount.

#### 2.1.4. Selective Reductive-Defluorination/Aromatization (RDF/A)

RDF/A of  $c\text{-}C_4F_8$  units next to aromatic structures is an enticing way of extending their conjugated  $\pi$  systems. For example, in the seven-step synthesis of perfluoropentacene, the last step involves reductive defluorination of a non-aromatic central ring with Zn dust at 280 °C to form a linearly conjugated acene [53]. As another example, a 360 °C reaction of TRPH with  $C_4F_8I_2$  in the presence of activated Cu powder produced small amounts of products of RDF/A, thereby extending the  $\pi$  system of TRPH by one aromatic ring containing a  $c\text{-}C_4F_4$  moiety [16]. Similarly, porphyrins with  $\omega\text{-}C_4F_8Cl$  substituents were converted into compounds with extended  $\pi$  systems by cyclization and RDF/A in the presence of  $Na_2S_2O_4/NaHCO_3$  in DMSO solution [54].

The latter method of RDF/A appeared to be most suitable for 1-PHNZ  $(\omega$ -C<sub>4</sub>F<sub>8</sub>I) as it involves the cyclization step. However, the reaction of 1-PHNZ( $(\omega$ -C<sub>4</sub>F<sub>8</sub>I) with Na<sub>2</sub>S<sub>2</sub>O<sub>4</sub>/NaHCO<sub>3</sub> in DMSO under the conditions described in ref. [52]. only yielded 1-PHNZ( $\omega$ -C<sub>4</sub>F<sub>8</sub>H) in quantitative yield. We therefore decided to first prepare the cyclized products as

$$C_{4}F_{8}I_{2} / 120-160 °C$$

$$solvent / Cu$$

$$PHNZ$$

$$C_{4}F_{8}I_{2} / hv / RT$$

$$PC / base / dry MeCN$$

$$PHNZ / C_{4}F_{8}I_{2} / hv / RT$$

$$PC / base / dry MeCN$$

$$F / F$$

$$Z_{3}-PHNZ(c-C_{4}F_{8})$$

Fig. 3. Simplified scheme summarizing the synthetic methodology developed in this work for the preparation of fluorinated azaacenes (PC = photochemical catalyst).

described in the previous chapter, and then apply the method from ref. [55]. using Zn dust for high-temperature RDF/A (Fig. 3). For this, a mixture of 1,2-PHNZ(c-C<sub>4</sub>F<sub>8</sub>) and 2,3-PHNZ(c-C<sub>4</sub>F<sub>8</sub>) was ground with zinc dust in a mortar under an Ar atmosphere, sealed under vacuum in a glass ampoule, and heated at 200 °C for 1 h. After the reaction, in order to avoid material loss, the complete ampoule containing the reaction products was ground to a fine powder and transferred to a temperature-gradient sublimation apparatus. The RDF/A compounds 1, 2-PHNZ(c-C<sub>4</sub>F<sub>4</sub>) and 2,3-PHNZ(c-C<sub>4</sub>F<sub>4</sub>) could be easily separated from each other with a combined 98% isolated yield. GCMS analysis showed that trace amounts of over-reduced species PHNZ(\omega-C\_4F\_3H) were also present (several isomers). These minor impurities were removed chromatographically to further purify the desired products. When solutions of 2,3-PHNZ(c-C<sub>4</sub>F<sub>4</sub>) in acetonitrile were left standing in the daylight for a couple of days, crystals formed with slightly shifted NMR signals. As will be described in chapter 2.2.5., this is a dimeric compound, presumably formed by photochemical [4+4] cycloaddition.

#### 2.1.5. Attempts on Using Directing Groups

A general problem of the substitution reaction at the phenazine

backbone is the regioselectivity of the reaction. As the linearly annelated (aza) arenes show smaller bandgaps than the bent ones, it would be advantageous to have a route to selectively obtain the former. A straightforward approach is blocking the sites, at which a substitution should be avoided, by other substituents, such as  $CH_3$  or  $CF_3$  groups. We chose the latter approach, because the strong acceptor 1,4,6,9-PHNZ( $CF_3$ )4 (compound K in Fig. 1; EA = 2.9 eV [14]) was not only available in our laboratories, but also would result in an extremely electron deficient system, which would be inherently interesting. A photochemical reaction was performed in the capillary flow reactor using Reaction P5 conditions, the optimized conditions for adding c- $C_4F_8$  to PHNZ. However, no products were formed: the starting material 1,4,6,9-PHNZ ( $CF_3$ )4 was recovered unaltered. At this stage, we can only speculate whether the desired reaction was either hampered by electronic or by steric effects.

We also tested if the regiospecificity of the reaction of PHNZ with  $C_4F_8I_2$  can be improved by introducing bulky protecting groups at the N atoms, thereby directing  $\omega$ - $C_4F_8I$  and/or c- $C_4F_8$  groups to the C2, C3, C7, and/or C8 positions. We synthesized 5,10-dihydroPHNZ(*tert*-butyl carboxylate)<sub>2</sub> (DiBocPHNZ; see ESI) and reacted it with  $C_4F_8I_2$  under

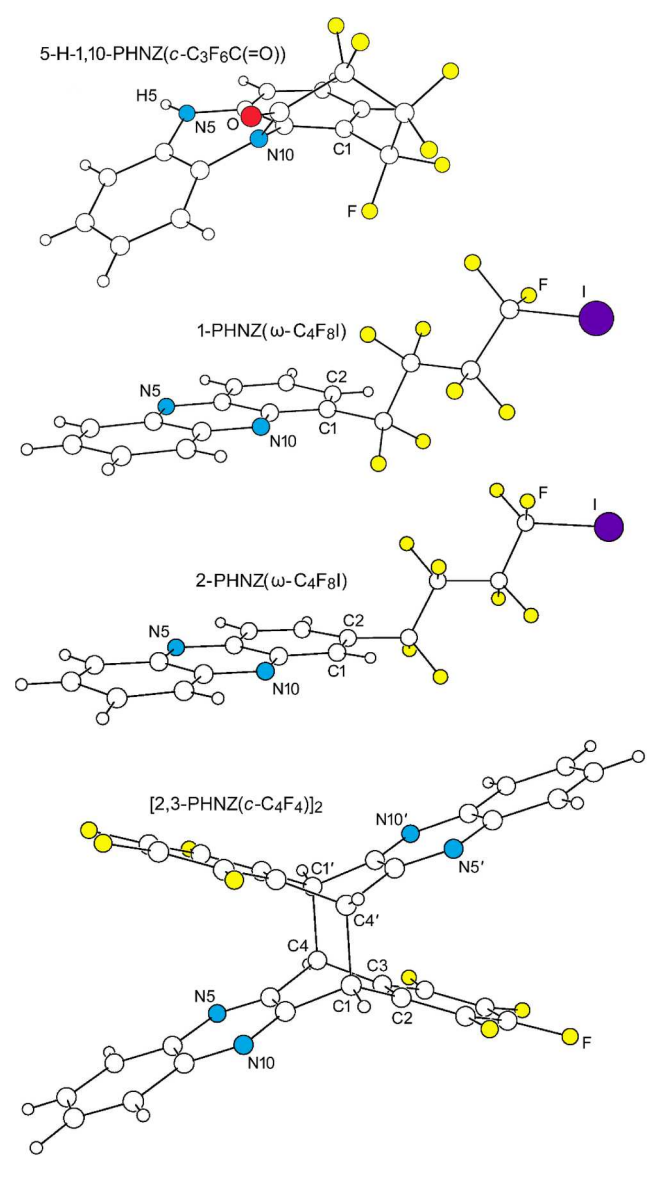


Fig. 4. X-ray diffraction determined molecular structures of (top to bottom) 5-H-1,10-PHNZ(c-C<sub>3</sub>F<sub>6</sub>C(=O)), 1-PHNZ( $\omega$ -C<sub>4</sub>F<sub>8</sub>I), 2-PHNZ( $\omega$ -C<sub>4</sub>F<sub>8</sub>I), and [2,3-PHNZ(c-C<sub>4</sub>F<sub>4</sub>)]<sub>2</sub>.

Reaction P5 conditions. The starting material lost its Boc groups upon photoirradiation, producing unsubstituted PHNZ, and the photochemical reaction then proceeded as previously observed with PHNZ.

#### 2.2. Molecular structures and solid-state packing

#### 2.2.1. Preliminary Comments

Four of the PHNZ derivatives prepared in this study were structurally characterized by X-ray diffraction techniques, i.e. 1-PHNZ(\omega-C\_4F\_8I), 2- $PHNZ(\omega-C_4F_8I), \quad [2,3-PHNZ(c-C_4F_4)]_2, \quad and \quad 5-H-1,10-PHNZ(c-C_3F_6C_4F_4)]_2$ (=O)). For convenience, we will continue to refer to them as substituted PHNZ derivatives, even though [2,3-PHNZ(c-C<sub>4</sub>F<sub>4</sub>)]<sub>2</sub> is the [4+4] cycloaddition dimer of 7,8,9,10-tetrafluoro-5,12-diazatetracene and 5-H-1,10-PHNZ(c-C<sub>3</sub>F<sub>6</sub>C(=O)) is a derivative of 5,10-dihydrophenazine. Drawings of the molecular structures of the four compounds are shown in Fig. 4. The relationships of the molecules to one another can be readily seen because they are oriented the same way in the four drawings: 1-PHNZ( $\omega$ -C<sub>4</sub>F<sub>8</sub>I) and 2-PHNZ( $\omega$ -C<sub>4</sub>F<sub>8</sub>I) are isomers that differ in the position of the ω-C<sub>4</sub>F<sub>8</sub>I substituent; 1-PHNZ(ω-C<sub>4</sub>F<sub>8</sub>I) is an intermediate in the formation of 5-H-1,10-PHNZ(c-C<sub>3</sub>F<sub>6</sub>C(=O)), as discussed before; and 2-PHNZ(ω-C<sub>4</sub>F<sub>8</sub>I) is an intermediate in the formation of [2,3-PHNZ $(c-C_4F_4)$ ]<sub>2</sub>, as also discussed before. The molecular structure of 2-PHNZ( $\omega$ -C<sub>4</sub>F<sub>8</sub>I) was determined by powder X-ray diffraction (see ESI for details). The other structures were determined by single-crystal X-ray diffraction (SCXRD) using synchrotron radiation on NSF's Chem-MatCARS beamline 15ID-D at the Advanced Photon Source at Argonne National Laboratory. The data were collected using a diamond {111} monochromator, selecting an X-ray wavelength of 0.41328 Å (standard wavelength). Unit cell parameters were determined by the least squares fit of the angular coordinates of all reflections. Integrations of all frames were performed using APEX III Suite software, and the structures were solved using SHELXTL/OLEX 2 software. Data collection and refinement parameters for the SCXRD structures are listed in Table 3. In addition, thermal ellipsoid plots are shown in ESI Figures S10 and S12-S14.

## 2.2.2. Structure of 2-PHNZ( $\omega$ -C<sub>4</sub>F<sub>8</sub>I)

As can be seen in Fig. 5, top, the PHNZ core remains almost planar upon substitution, with a mean deviation of the  $14~\rm sp^2$  atoms from the least-squares plane of  $\pm 0.011$  Å. The same figure shows that the planar molecules are stacked along the crystallographic b axis such that (i) their least-squares planes are rigorously parallel and (ii) each molecule has a

different degree of overlap with the  $\pi$  system of its nearest neighbors along the stack Fig. 6, top, shows parallel projection drawings of the  $\pi-\pi$  overlap of neighboring pairs of stacked molecules. In the top pair of molecules, the perpendicular out-of-plane displacements (OOPDs, see ref. [56]. for a definition) of the five atoms directly below the least-squares plane of the upper molecule range from 3.47 to 3.51 Å and average 3.49 Å. In the bottom pair of molecules, the OOPDs of the two atoms below the plane of the upper molecule are 3.57 and 3.62 Å. These distances are larger than the ca.  $3.35\pm0.05$  Å distances observed in graphite [57] and many other PAHs [58], but they are in line with the 3.46–3.52 Å distances observed in  $\alpha$ -PHNZ [59] and  $\beta$ -PHNZ [60], as shown in Figure S15.

## 2.2.3. Structure of 1-PHNZ( $\omega$ -C<sub>4</sub>F<sub>8</sub>I)

Just like in 2-PHNZ( $\omega$ -C<sub>4</sub>F<sub>8</sub>I), the 14 sp<sup>2</sup> atoms of the PHNZ core in 1-PHNZ(ω-C<sub>4</sub>F<sub>8</sub>I) lie in one plane with a mean deviation from their leastsquares plane of  $\pm 0.022$  Å Fig. 5, bottom, shows that the planar molecules are stacked along the crystallographic a axis such that (i) their least-squares planes are rigorously parallel and (ii) each molecule has a different degree of overlap with the  $\pi$  system of its nearest neighbors along the stack Fig. 6, bottom, shows parallel projection drawings of the  $\pi$ - $\pi$  overlap of neighboring pairs of stacked molecules. In the left pair of molecules, the perpendicular OOPDs of the atoms directly below the least-squares plane of the upper molecule range from 3.28 to 3.35 Å and average 3.30 Å. In the right pair of molecules, the OOPDs range from 3.36 to 3.42 Å and average 3.39 Å. These intermolecular spacings are significantly smaller than the 3.5–3.6 Å spacings in 2-PHNZ(ω-C<sub>4</sub>F<sub>8</sub>I) and the two polymorphs of unsubstituted PHNZ. As a consequence, the intermolecular  $\pi$ - $\pi$  interactions in crystalline 1-PHNZ( $\omega$ -C<sub>4</sub>F<sub>8</sub>I) may be significantly stronger than those in crystalline 2-PHNZ(ω-C<sub>4</sub>F<sub>8</sub>I),  $\alpha$ -PHNZ, and  $\beta$ -PHNZ. There is precedent for small intermolecular spacings in PHNZ derivatives, e.g. 1,2-PHNZ(c-C<sub>4</sub>F<sub>4</sub>), shown in Figure S15, with an average  $\pi$ – $\pi$  OOPDs that average 3.30 Å [24].

Fig. 7 shows the solid-state packings in the structures of 1-PHNZ  $(\omega\text{-}C_4F_8I)$  and 2-PHNZ( $\omega\text{-}C_4F_8I)$ . Both exhibit fluorous domains and hydrocarbon domains. However, the packing in 1-PHNZ( $\omega\text{-}C_4F_8I)$  appears to be more compact than in 2-PHNZ( $\omega\text{-}C_4F_8I)$ , which results in crystalline 1-PHNZ( $\omega\text{-}C_4F_8I)$  having a 6.2% higher density (2.095 g cm $^{-3}$ ) than crystalline 2-PHNZ( $\omega\text{-}C_4F_8I)$  (1.972 g cm $^{-3}$ ). The drawings in the middle of Fig. 7 highlight the differences in the shapes of these two isomers (i.e., more compact vs. more elongated). The difference in

**Table 3**Data collection and final parameters for the refined structures.

compound	$1\text{-PHNZ}(\omega\text{-C}_4F_8I)^a$	$5-H-1,10-PHNZ(c-C_3F_6C(=O))^a$	$[2,3-PHNZ(c-C_4F_4)]_2^a$	$2\text{-PHNZ}(\omega\text{-C}_4F_8I)^b$
formula unit	$C_{16}H_7F_8IN_2$	C <sub>16</sub> H <sub>8</sub> F <sub>6</sub> N <sub>2</sub> O	C <sub>32</sub> H <sub>12</sub> F <sub>8</sub> N <sub>4</sub>	C <sub>16</sub> H <sub>7</sub> F <sub>8</sub> IN <sub>2</sub>
formula wt., g mol <sup>-1</sup>	506.14	358.24	604.46	506.14
habit, color	needle, yellow	plate, colorless	block, brown	unknown, yellow
crystal system	triclinic	triclinic	monoclinic	Monoclinic
space group, Z	P-1, 2	P-1, 4	$P2_1/c, 2$	P2 <sub>1</sub> /n, 4
a, Å	6.678(4)	11.382(8)	6.8096(5)	5.87503(17)
b, Å	9.998(6)	11.575(6)	14.5960(11)	10.23186(29)
c, Å	12.976(6)	11.864(6)	12.0958(9)	28.36695(64)
$\alpha$ , deg	70.397(16)	82.484(14)	90	90
$\beta$ , deg	79.72(2)	83.17(2)	97.250(1)	91.6296(19)
γ, deg	84.00(2)	65.532(17)	90	90
<i>V</i> , Å <sup>3</sup>	802.1(8)	1406.8(14)	1192.63(15)	1704.518(79)
$ ho_{ m calc}$ , g cm $^{-3}$	2.095	1.691	1.683	1.972
T, K	100(2)	100(2)	100(2)	293
$R(F) (I > 2\sigma(I))^{c}$	0.0247	0.0439	0.0420	$R_{Bragg}^{d}$ 0.0208
$wR(F^2)$ [all data] <sup>c</sup>	0.0907	0.1332	0.1860	$R_{wp}^{d}$ 0.0319
GOF <sup>c</sup>	1.163	1.094	1.050	GOF <sup>d</sup> 1.971
C-C bond precision, Å	0.0017	0.0020	0.0021	0.0142

Abbreviations: PHNZ = phenazine.

<sup>&</sup>lt;sup>a</sup>Single crystal X-ray diffraction.

<sup>&</sup>lt;sup>b</sup>Powder X-ray diffraction.

 $<sup>{}^{</sup>c}R(F) = \Sigma ||F_{o}| - |F_{c}|| / \Sigma |F_{o}|; wR(F^{2}) = (\Sigma [w(F_{o}^{2} - F_{c}^{2})^{2}] / \Sigma [w(F_{o}^{2})^{2}])^{1/2}; GOF = (\Sigma [w(F_{o}^{2} - F_{c}^{2})^{2}] / (N - P))^{1/2}.$ 

 $<sup>{}^{</sup>d}R_{Bragg} = \Sigma ||I_{o,k}| - |I_{c,k}|| / \Sigma |I_{o,k}|; R_{wp} = (\Sigma [w_m(Y_{o,m}^2 - Y_{c,m}^2)^2] / \Sigma [w_mY_{o,m}^2])^{1/2}; GOF = (\Sigma [w_m(Y_{o,m}^2 - Y_{c,m}^2)^2] / (M - N))^{1/2}.$ 

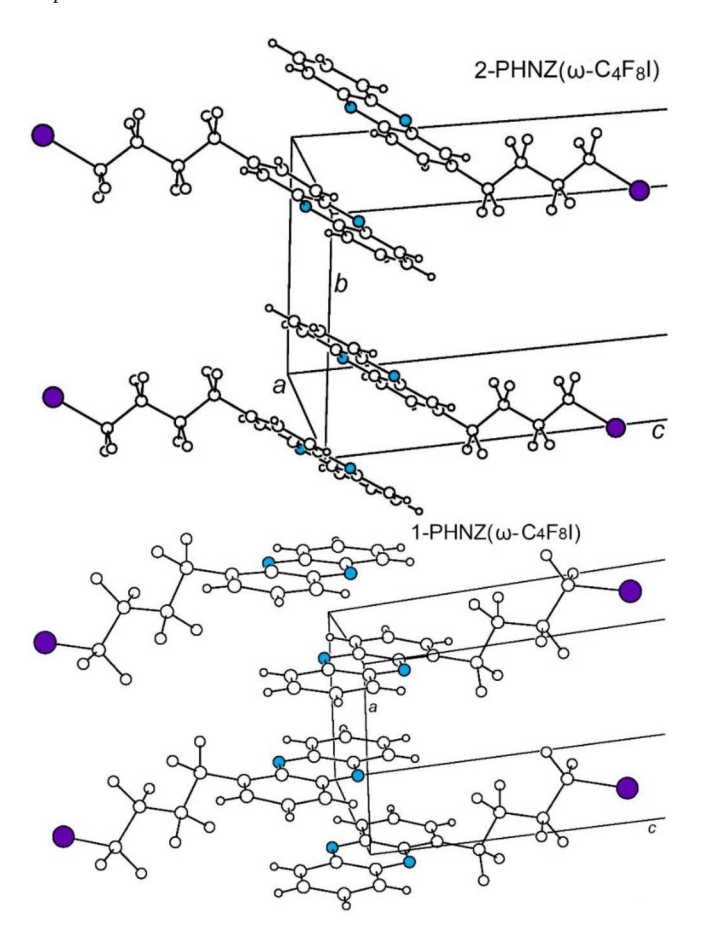
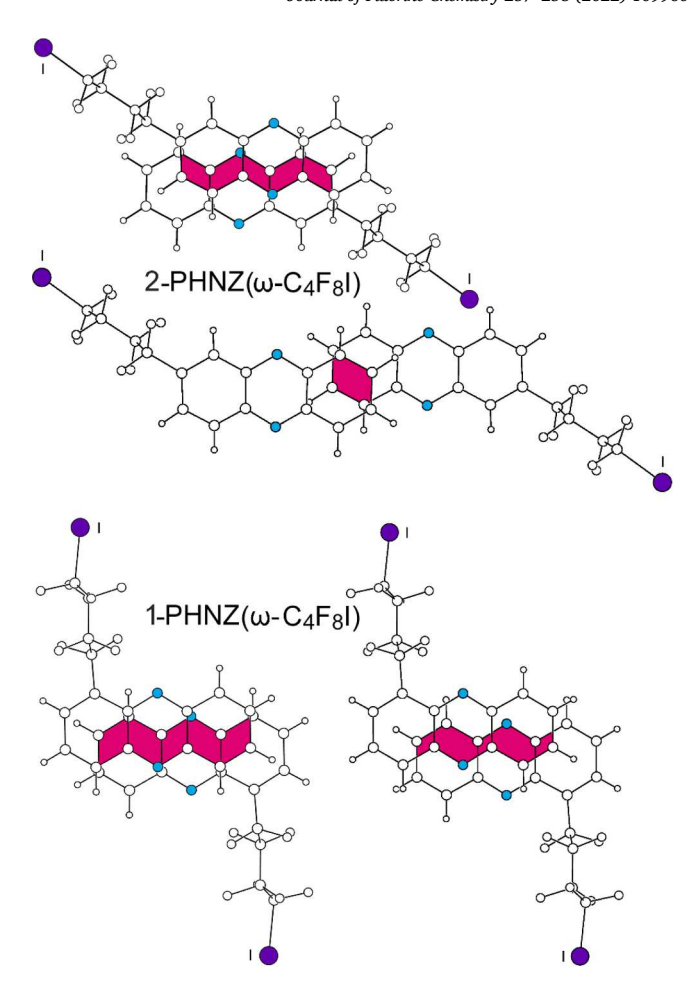


Fig. 5. Top: A portion of the structure of 2-PHNZ( $\omega$ -C<sub>4</sub>F<sub>8</sub>I), showing the offset pairs of  $\pi$ -stacked molecules along the crystallographic b axis (the N and I atoms are shaded blue and violet, respectively). The N•••N centroids of every other molecule define the unit cell b axis. The PHNZ core is planar, with a mean displacement of the 14  $sp^2$  atoms from their least-squares plane of  $\pm 0.011\ \mbox{\normalfont\AA}.$ The least-squares planes of the PHNZ cores of neighboring molecules are rigorously parallel. Each molecule has a significantly different degree of  $\pi$ - $\pi$ overlap with its nearest neighbor molecules. This is shown in more detail in Fig. 6. Bottom: A portion of the structure of 1-PHNZ(ω-C<sub>4</sub>F<sub>8</sub>I), showing the offset pairs of  $\pi$ -stacked molecules along the crystallographic  $\alpha$  axis (the N and I atoms are shaded blue and violet, respectively). The N•••N centroids of every other molecule define the unit cell a axis. The PHNZ core is planar, with a mean displacement of the 14 sp<sup>2</sup> atoms from their least-squares plane of  $\pm 0.022$  Å. The least-squares planes of the PHNZ cores of neighboring molecules are rigorously parallel. Each molecule has significantly different  $\pi$ – $\pi$  overlaps with its two nearest neighbor molecules, which is shown in more detail in Fig. 6.

density may also result from differences in the networks of intermolecular N•••I and F•••F interactions, which are shown in Fig. 8. In 1-PHNZ  $(\omega$ -C<sub>4</sub>F<sub>8</sub>I), the N•••I distance is 3.055(2) Å and the shortest F•••F distances are 2.801(2) and 3.105(2) Å. In 2-PHNZ( $\omega$ -C<sub>4</sub>F<sub>8</sub>I), the N•••I distance, at 3.15(1) Å, is longer than in 1-PHNZ( $\omega$ -C<sub>4</sub>F<sub>8</sub>I), and the F•••F distances, at 3.09(1) and 3.10(1) Å, are also longer than in 1-PHNZ (ω-C<sub>4</sub>F<sub>8</sub>I). The C–I•••N angles are 175° in 1-PHNZ(ω-C<sub>4</sub>F<sub>8</sub>I) and 167° in 2-PHNZ(ω-C<sub>4</sub>F<sub>8</sub>I). The N•••I distances are considerably shorter than the 3.53 Å sum of van der Waals radii for N (1.55 Å) and I (1.98 Å) [61], what might be a hint for halogen bonding [62]. However, in both compounds the N•••I distances are longer than the 2.84(3) Å distance in the co-crystal structure of  $1.4-C_4F_8I_2$  and bipyridine [63], in which the iodoperfluoroalkyl and aromatic amine moieties are in separate molecules (the C-I•••N angle, at 177.5(4)°, is also close to linear) [61]. The larger N•••I distances in 1-PHNZ(ω-C<sub>4</sub>F<sub>8</sub>I) and 2-PHNZ(ω-C<sub>4</sub>F<sub>8</sub>I) may be because the  $\pi$ - $\pi$  stacking of PHNZ moieties prevents optimal C-I•••N halogen bonding.



**Fig. 6.** Parallel projection drawings of the  $\pi$ - $\pi$  overlap (shaded magenta) of neighboring pairs of stacked molecules in the structure of 2-PHNZ( $\omega$ -C<sub>4</sub>F<sub>8</sub>I) (left) and 1-PHNZ( $\omega$ -C<sub>4</sub>F<sub>8</sub>I) (right). In the top pair of 2-PHNZ( $\omega$ -C<sub>4</sub>F<sub>8</sub>I) molecules, the perpendicular out-of-plane displacements (OOPDs) of the five atoms directly below the plane of the upper molecule range from 3.47 to 3.51 Å and average 3.49 Å. In the bottom pair of 2-PHNZ( $\omega$ -C<sub>4</sub>F<sub>8</sub>I) molecules, the OOPDs of the two atoms below the plane of the upper molecule are slightly larger, 3.57 and 3.62 Å. In the left pair of 1-PHNZ( $\omega$ -C<sub>4</sub>F<sub>8</sub>I) molecules, the OOPDs of the atoms directly below the plane of the upper molecule range from 3.29 to 3.33 Å and average 3.31 Å. In the right pair of 1-PHNZ( $\omega$ -C<sub>4</sub>F<sub>8</sub>I) molecules, the OOPDs range from 3.33 and 3.37 Å and average 3.35 Å.

#### 2.2.4. Structure of 5-H-1,10-PHNZ(c- $C_3F_6C(=O)$ )

There are two nearly identical molecules of 5-H-1,10-PHNZ(c-C<sub>3</sub>F<sub>6</sub>C (=O)) in the asymmetric unit (only one is shown in Fig. 4, top, as well as the other figures). The triclinic centrosymmetric unit cell contains these two molecules and their enantiomers (P-1, Z = 4) Fig. 9 shows that this cyclic amide is formally a derivative of dihydrophenazine (H<sub>2</sub>PHNZ, bottom [64]). It is presumably formed from 1-PHNZ( $\omega$ -C<sub>4</sub>F<sub>8</sub>I) by a sequence of reactions involving (i) homolytic scission of the C–I bond, (ii) electrophilic attack at N10 under formation of the F<sub>2</sub>C–N bond and thus the seven membered ring, (iii) addition of an H atom to N5, and (iv) conversion of the CF<sub>2</sub> moiety attached to N10 into a C=O carbonyl group (potentially by hydrolysis with traces of water either from the solvent or the glass wall), not necessarily in that order.

The C=O bond distances in the two molecules of 5-H-1,10-PHNZ(c-C<sub>3</sub>F<sub>6</sub>C(=O)) are 1.220(2) and 1.231(2) Å, confirming the sp<sup>2</sup> hybridization of the C atoms. The molecule shown in Fig. 9 is folded at the N5•••N10 hinge by 30.5° (the fold angle in the other molecule in the asymmetric unit is 33.8°). The N–C distances within the dihydrophenazine moieties of both molecules range from 1.389(2) to 1.444 (2) Å, confirming the sp<sup>3</sup> hybridization of the N atoms (note that the N

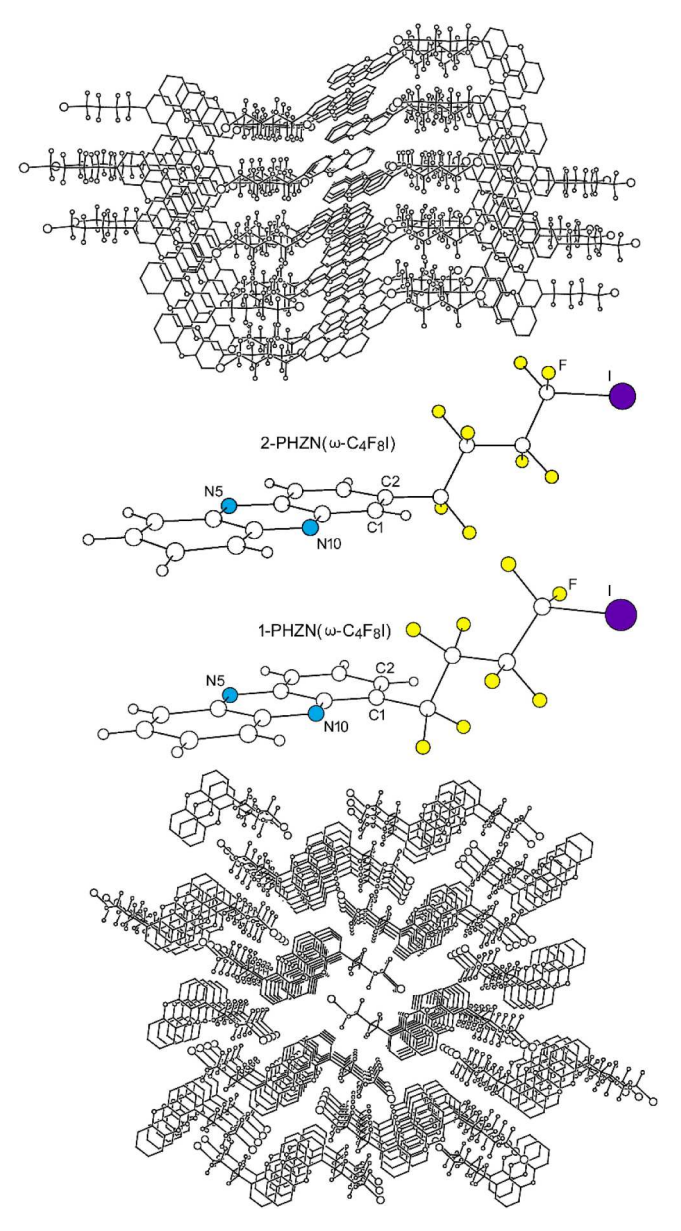


Fig. 7. Packing of molecules in the X-ray structures of 2-PHNZ( $\omega$ -C<sub>4</sub>F<sub>8</sub>I) (top) and 1-PHNZ( $\omega$ -C<sub>4</sub>F<sub>8</sub>I) (bottom). Hydrogen atoms have been removed for clarity. The molecular structures in the middle of the figure demonstrate that the shapes of these constitutionally similar molecules are significantly different.

(sp²)–C distances in 1- PHNZ( $\omega$ -C<sub>4</sub>F<sub>8</sub>I) range from 1.3357(14) to 1.3443 (13) Å). For comparison, the fold angles in crystalline H<sub>2</sub>PHNZ [59] and dihydroanthracene [65] are 21.5 and 36.6°, respectively, and the N (sp³)–C distances in H<sub>2</sub>PHNZ range from 1.4015(16) to 1.4138(17) Å. The greater fold angle in 5-H-1,10-PHNZ(c-C<sub>3</sub>F<sub>6</sub>C(=O)) relative to H<sub>2</sub>PHNZ is probably due to the constraints imposed by formation of the seven-membered ring.

The conformations of the seven-membered ring in 5-H-1,10-PHNZ(c-C<sub>3</sub>F<sub>6</sub>C(=O)) and the seven-membered ring in  $\epsilon$ -caprolactam [63] are compared in ESI Figure S17. Given the presence of the six F atoms, two additional C(sp<sup>2</sup>) atoms in the ring, and the inclusion of the N atom in another ring, the conformations are quite similar. The five atoms that comprise the O-C-N-C moieties are approximately planar (the average deviation of these atoms from their least-squares plane is only 0.04 Å). Accordingly, the two O-C-N-C torsion angles, at 5.3° and 9.3°, are relatively small.

The network of C=O•••H-N hydrogen bonds in 5-H-1,10-PHNZ(c-

 $C_3F_6C(=0)$ ) is shown in Fig. 10. The O•••H, and O•••N distances and O•••H–N angle are 2.06 Å, 2.976(2) Å, and 171°, respectively, for one of the two unique hydrogen bonds and 2.08 Å, 2.957(2) Å, and 168°, respectively, for the other hydrogen bond. There is no intermolecular  $\pi$ – $\pi$  distance shorter than 3.7 Å in this structure.

#### 2.2.5. Structure of $[2,3-PHNZ(c-C_4F_4)]_2$

This [4+4] cycloaddition dimer, shown in Fig. 4, presumably formed by photochemical cycloaddition in solution from the planar, monomeric 2,3-PHNZ(c-C<sub>4</sub>F<sub>4</sub>) (formally 7,8,9,10-tetrafluoro-5,12-diazatetracene), which is an isomer of the planar, structurally characterized compound tetrafluorobenzo[a]phenazine [24] shown in ESI Figure S16.

Fig. 11 shows a comparison of [2,3-PHNZ(c-C<sub>4</sub>F<sub>4</sub>)]<sub>2</sub> with the [4+4] cycloaddition dimer [tetraazatetracene(C = C-TIPS)<sub>2</sub>]<sub>2</sub> [66]. The fold angles are 41.3° in [2,3-PHNZ(c-C<sub>4</sub>F<sub>4</sub>)]<sub>2</sub> and 45.1° in [tetraazatetracene (C = C-TIPS)<sub>2</sub>]<sub>2</sub>. The bridgehead–bridgehead  $C(sp^3)$ - $C(sp^3)$  bonds in these centrosymmetric dimers are 1.618(2) Å in [2,3-PHNZ(c-C<sub>4</sub>F<sub>4</sub>)]<sub>2</sub> and 1.591(8) Å in [tetraazatetracene(C = C-TIPS)<sub>2</sub>]<sub>2</sub> Fig. 12 shows the packing of the dimeric molecules in the structure of [2,3-PHNZ(c-C<sub>4</sub>F<sub>4</sub>)]<sub>2</sub>. The shortest intermolecular F•••F contacts are 2.843(2) Å. There is no intermolecular  $\pi$ - $\pi$  overlap in this structure.

#### 2.3. Electrochemical Reduction Potentials

One of the goals of this work was to prepare stable, robust molecules as candidates for organic electronic devices that possess strong electron acceptor properties, while they tend to stack with significant intermolecular  $\pi$ - $\pi$  overlap when crystallized. Planar acenes such as ANTH and TETR with F atoms and/or fluorous substituents are possible candidates. However, heteroacenes such as PHNZ and 5,12-diazatetracene (5,12-DAZT) would be even better starting materials because they are stronger electron acceptors than their hydrocarbon analogs. For example, the gas-phase electron affinities (*EAs*) of ANTH and PHNZ are 0.53(2) [67] and 1.31(10) eV [68], respectively, and the first reduction potentials,  $E_{1/2}(0/-)$  values, from cyclic voltammetry in 1,2-dimethoxyethane (DME) solution are -2.52 [11] and -1.74 V vs. FeCp<sub>2</sub>+ $^{1/0}$  [14], respectively. As another example,  $E_{1/2}(0/-)$  values for TETR and 5,12-DAZT are -1.60 (DMF solution) [69,70] and -1.44 V (THF solution) vs. FeCp<sub>2</sub>+ $^{1/0}$  [71], respectively.

The  $E_{1/2}(0/-)$  values) for PHNZ, fluorinated PHNZ derivatives, and related compounds are listed in Table 4 [14,24,24,66]. Nine values are for new compounds prepared in this work. Selected cyclic voltammograms are shown in Figs. 13 and 14. The results reveal the relative electron-withdrawing effects of F atoms and CF<sub>3</sub>, n-C<sub>4</sub>F<sub>8</sub>I, c-C<sub>4</sub>F<sub>4</sub>, and c-C<sub>4</sub>F<sub>8</sub> groups, as well as the effects of putting these substituents in different positions on PHNZ and 5,12-DAZT. All of the perfluoroalkyl electron-withdrawing substituents resulted in  $E_{1/2}(0/-)$  values that are cathodically shifted relative to  $E_{1/2}(0/-)$  for unsubstituted PHNZ by as much as 0.58 V for a single c-C<sub>4</sub>F<sub>8</sub> group. The cathodic shifts will be referred to as  $\Delta E_{1/2}(0/-)$  values.

One must be circumspect when comparing  $E_{1/2}(0/-)$  values in different solvents. The DMF vs. THF  $E_{1/2}(0/-)$  values and the CH<sub>2</sub>Cl<sub>2</sub> vs. CH<sub>3</sub>CN  $E_{1/2}(0/-)$  values for a number of aromatic compounds only differ by 0.02-0.03 V [72-74]. However, the CH2Cl2 vs. CH3CN and the DME vs. CH<sub>3</sub>CN  $E_{1/2}(0/-)$  values for PHNZ differ by 0.16 and 0.12 V, respectively (see Table 4). A recent theoretical study reported DFT-predicted  $E_{1/2}(0/-)$  values for PHNZ that varied by as much as 0.6 V depending on the dielectric constant of the solvent (see ESI Figure S23) [75]. The calculations did not include the dielectric decrement due to the supporting electrolyte, which could make the differences in effective dielectric constants of 0.1 M solutions of N(n-Bu)<sub>4</sub>PF<sub>6</sub> in various solvents smaller than the intrinsic differences of the pure solvent [76,77]. For example, the DFT-predicted CH<sub>2</sub>Cl<sub>2</sub> vs. CH<sub>3</sub>CN  $E_{1/2}(0/-)$ values for PHNZ differ by 0.16 V [70], the same as the difference in the experimental values, but the DFT-predicted DME vs.  $CH_3CN\ E_{1/2}(0/-)$ values for PHNZ differ by 0.23 V [70], nearly twice as large as the

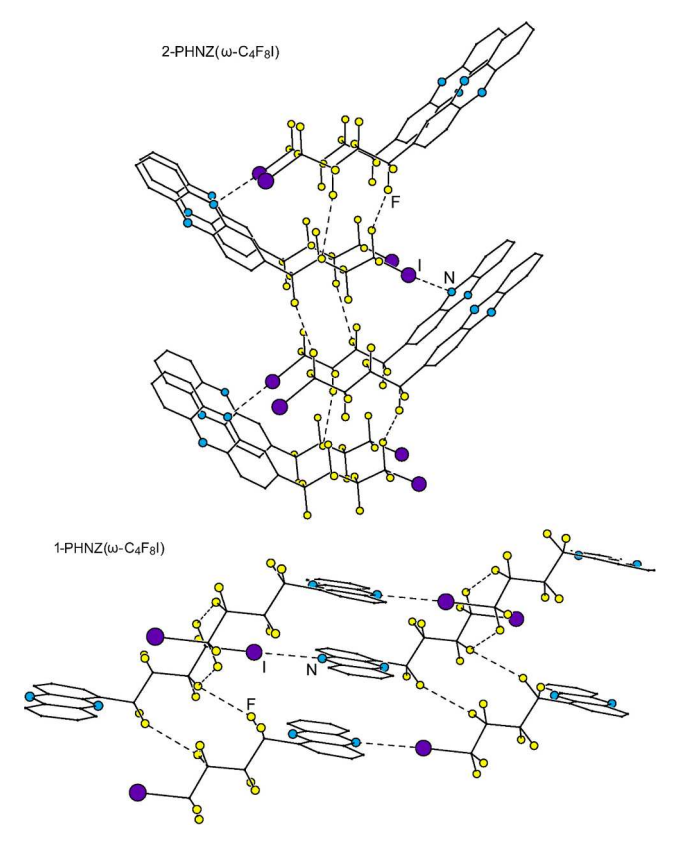


Fig. 8. Drawings of portion of the structures of 2-PHNZ( $\omega$ -C<sub>4</sub>F<sub>8</sub>I) (top) and 1-PHNZ( $\omega$ -C<sub>4</sub>F<sub>8</sub>I) (bottom) showing the networks of intermolecular N•••I and F•••F interactions (H atoms removed for clarity). In 2-PHNZ( $\omega$ -C<sub>4</sub>F<sub>8</sub>I), the N•••I distance is 3.15(1) Å and the shortest F•••F distances are 3.09(1) and 3.10(1) Å. In 1-PHNZ( $\omega$ -C<sub>4</sub>F<sub>8</sub>I), the N•••I distance is 3.055(2) Å and the shortest F•••F distances are 2.801(2) and 3.105(2) Å. The C-I•••N angles are 167° in 2-PHNZ( $\omega$ -C<sub>4</sub>F<sub>8</sub>I) and 175° in 1-PHNZ( $\omega$ -C<sub>4</sub>F<sub>8</sub>I).

difference in experimental values (see Table 4). Therefore, it is probably more meaningful to compare  $\Delta E_{1/2}(0/-)$  values in different solvents than to compare  $E_{1/2}(0/-)$  values. Note that the  $\Delta E_{1/2}(0/-)$  values for 1, 2-PHNZ(c-C<sub>4</sub>F<sub>8</sub>) in CH<sub>3</sub>CN and CH<sub>2</sub>Cl<sub>2</sub>, which are 0.18 and 0.15 V, respectively, are essentially the same.

The c-C<sub>4</sub>F<sub>8</sub> group produced about the same  $\Delta E_{1/2}(0/-)$  value (0.58 and 0.48 V for 2,3- and 1,2-PHNZ(c-C<sub>4</sub>F<sub>8</sub>), respectively) as a pair of CF<sub>3</sub> groups (0.53 V for the isomers of PHNZ(CF<sub>3</sub>)<sub>2</sub> [14]). The reason for the 100 mV difference in  $\Delta E_{1/2}(0/-)$  values for the two PHNZ(c-C<sub>4</sub>F<sub>8</sub>) isomers is not known at this time. It may be due to the different dipole moments of these isomers and the concomitant greater stabilization of negative charge on the "linear" 2,3- isomer than on the "bent" 1,2- isomer. The effect is consistent with the 80 mV greater  $\Delta E_{1/2}(0/-)$  for the "linear-bent" isomer 1,2,7,8-PHNZ(c-C<sub>4</sub>F<sub>8</sub>)<sub>2</sub> relative to the "bent-bent" isomer 1,2,6,7-PHNZ(c-C<sub>4</sub>F<sub>8</sub>)<sub>2</sub> [24] and the 50 mV greater  $\Delta E_{1/2}(0/-)$  value for polar 1,3,6,9-PHNZ(CF<sub>3</sub>)<sub>4</sub> relative to nonpolar 1,4,6,9-PHNZ (CF<sub>3</sub>)<sub>4</sub> [14].

The c-C<sub>4</sub>F<sub>4</sub> group induced significantly smaller  $\Delta E_{1/2}(0/-)$  values, 0.26 and 0.18 V for 2,3- and 1,2-PHNZ(c-C<sub>4</sub>F<sub>4</sub>), respectively, than the C<sub>4</sub>F<sub>8</sub> group, 0.58 and 0.48 V for 2,3- and 1,2-PHNZ(c-C<sub>4</sub>F<sub>8</sub>), respectively. The PHNZ(c-C<sub>4</sub>F<sub>4</sub>) isomers are formally tetrafluoro derivatives of 5,12-DAZT and benzo[a]phenazine, respectively, and have an additional aromatic ring, and hence a larger  $\pi$  system than the PHNZ(c-C<sub>4</sub>F<sub>8</sub>) isomers. This is supported by the band gaps experimentally determined by UV/ vis spectroscopy (see ESI Figure S24 and Table S8): upon RDF/A, the band gap decreases form 3.18 eV to 2.99 eV in the 1,2 system and from 3.21 eV to 2.80 eV in the 2,3 system. Nevertheless, the PHNZ(c-C<sub>4</sub>F<sub>8</sub>) isomers have  $\Delta E_{1/2}(0/-)$  values that are more than twice as large as the PHNZ(c-C<sub>4</sub>F<sub>4</sub>) isomers. This may seem counterintuitive, especially in the case of 2,3-PHNZ(c-C<sub>4</sub>F<sub>8</sub>) vs. 2,3-PHNZ(c-C<sub>4</sub>F<sub>4</sub>), because, as explained

above, the PHNZ(c-C<sub>4</sub>F<sub>4</sub>) isomers have an additional aromatic ring. Acenes and heteroacenes generally become stronger electron acceptors as more aromatic rings are added (compare the  $E_{1/2}(0/-)$  values for PHNZ and 5,12-DAZT in Table 4, which are -1.78 and -1.44 V vs.  $\text{FeCp}_2^{+/0}$ , respectively, with the  $E_{1/2}(0/-)$  values for DMF solutions of ANTH, TETR, and pentacene (PENT), which are -2.39, -2.00, and -1.73 V vs. FeCp<sub>2</sub><sup>+/0</sup>, respectively [64], and the  $E_{1/2}(0/-)$  values for CH<sub>3</sub>CN solutions of perfluoroanthracene and perfluorotetracene, at, -1.29 and -0.84 V vs.  $FeCp_2^{+/0}$ , respectively [53]). This suggests that the C<sub>4</sub>F<sub>8</sub> substituent in 2,3-PHNZ(c-C<sub>4</sub>F<sub>8</sub>) more than compensates for the extra aromatic ring bearing four F atoms in 2,3-PHNZ(c-C<sub>4</sub>F<sub>4</sub>). Although an F atom is a stronger electron-withdrawing group than a perfluoroalkyl (R<sub>F</sub>) group when attached to a C(sp<sup>3</sup>) atom, F is a much weaker electron-withdrawing group than R<sub>F</sub> when attached to an aromatic  $C(sp^2)$  atom [63]. For example, the DFT predicted EAs of 2, 6-ANTH(CF<sub>3</sub>)<sub>2</sub> and 2,6-ANTH(F)<sub>2</sub> are 1.29 and 0.75 eV, respectively

The introduction of an additional aromatic ring does not always result in a stronger electron acceptor PAH. TETR is a much stronger electron acceptor than benzo[a]anthracene even though they both have four aromatic rings; their *EAs* are 1.06(1) [79] and 0.4(1) eV [80], respectively, and their  $E_{1/2}(0/-)$  values in DMF are -2.00 and -2.43 V vs. FeCp<sub>2</sub>+/0, respectively [64], a difference of 0.43 V. However, the  $\Delta E_{1/2}(0/-)$  values for 2,3- and 1,2-PHNZ(c-C<sub>4</sub>F<sub>4</sub>) are similar, 0.26 and 0.18 V, respectively, a difference of only 0.08 V, even though the hetero-PAH in 1,2-PHNZ(c-C<sub>4</sub>F<sub>4</sub>) is benzo[a]phenazine, the four rings of which match the four-ring pattern of the weak electron acceptor benzo [a]anthracene. Apparently, the difference in band gaps (2.99 eV and 2.80 eV, *vide infra*, thus  $\Delta E = 0.19$  eV) partly compensates for this effect. Therefore, it may be the case that benzo[a]phenazine and 5,12-DAZT

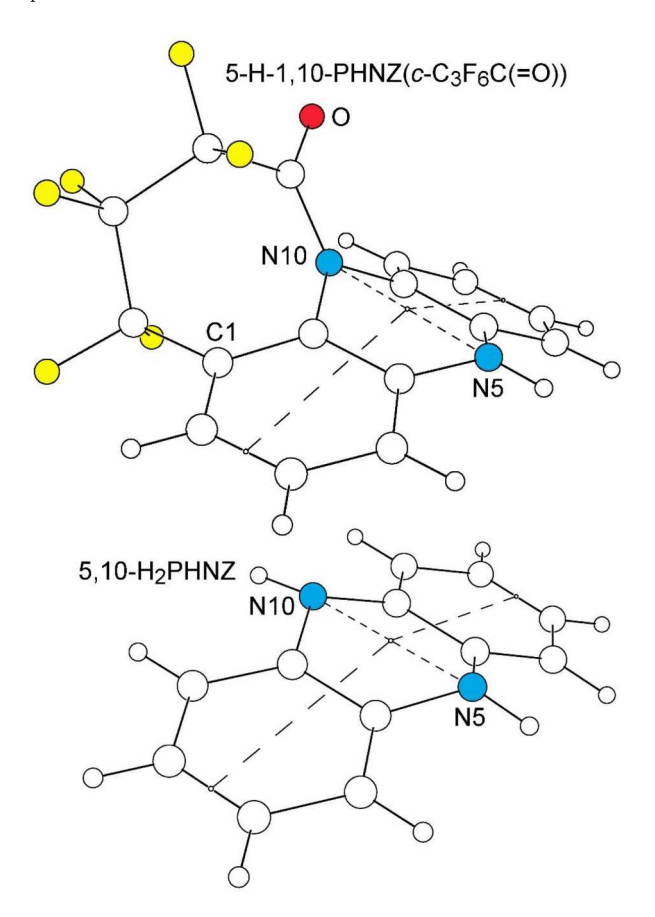


**Fig. 9.** (Top) The structure of 5-H-1,10-PHNZ(c-C<sub>3</sub>F<sub>6</sub>C(=O)), showing the  $30.5^{\circ}$  fold along the N5•••N10 hinge. The range of the four N–C distances is 1.389(2)–1.444(2) Å. (Bottom) The structure of 5,10-H<sub>2</sub>PHNZ (ref. [64].). The PHNZ core is folded by  $21.5^{\circ}$  at the N5•••N10 hinge. The range of the four N–C distances is 1.402(2)–1.414(2) Å. The greater fold angle in 5-H-1,10-PHNZ(c-C<sub>3</sub>F<sub>6</sub>C(=O)) is probably due to the constraints imposed by the seven-membered ring.

have similar *EA*s and  $E_{1/2}(0/-)$  values, unlike benzo[a]anthracene and ANTH.

A comparison of 1,2,3,4-(5,12-DAZT)F<sub>4</sub> and 7,8,9,10-(5,12-DAZT)F<sub>4</sub> (i.e., 1,2-PHNZ(c-C<sub>4</sub>F<sub>4</sub>)) is also of interest. Their  $\Delta E_{1/2}(0/-)$  values are similar, 0.19 [24] and 0.26 V (this work), respectively. This suggests that the 1,2,3,4 and the 7,8,9,10 C(sp<sup>2</sup>) atoms of 5,12-DAZT make essentially the same overall contribution to its LUMO, which is consistent with the DFT-predicted LUMO reported in a recently published theoretical study and shown in ESI Figure S25 [81].

The compounds 1- and 2-PHNZ(ω-C<sub>4</sub>F<sub>8</sub>I) are rare examples of PAH or hetero-PAH compounds with a single perfluoroalkyl-type substituent. The  $\Delta E_{1/2}(0/-)$  values, at 0.37 and 0.33 V, respectively, match the largest cathodic shifts, per  $R_F$  group, observed for a PAH $(R_F)_n$  or hetero-PAH(R<sub>F</sub>)<sub>n</sub> derivative. The  $\Delta E_{1/2}(0/-)$  values, per CF<sub>3</sub> group, for PHNZ (CF<sub>3</sub>)<sub>2</sub> (mixture of isomers), 1,3,6,9-PHNZ(CF<sub>3</sub>)<sub>4</sub>, 1,4,6,9-PHNZ(CF<sub>3</sub>)<sub>4</sub>, an isomer of perylene(CF<sub>3</sub>)<sub>4</sub> [11], an isomer of ANTH(CF<sub>3</sub>)<sub>5</sub> [11], and an isomer of naphthalene(CF<sub>3</sub>)<sub>4</sub> [73] are 0.26, 0.21, 0.19, 0.23, 0.25, and 0.37 V, respectively. Except for the naphthalene compound, the  $\Delta E_{1/2}(0/-)$  values for 1- and 2-PHNZ( $\omega$ -C<sub>4</sub>F<sub>8</sub>I) are more than 50% larger than the  $\Delta E_{1/2}(0/-)$  values per R<sub>F</sub> group than for the other compounds. The similar  $\Delta E_{1/2}(0/-)$  values for 1- and 2-PHNZ( $\omega$ -C<sub>4</sub>F<sub>8</sub>I) demonstrate that the C(sp<sup>2</sup>) orbital contributions to the PHNZ LUMO are essentially the same, in harmony with the recently reported DFT-predicted PHNZ LUMO shown in ESI Figure S25. Finally, although the first reductions of 1- and 2-PHNZ(\omega-C\_4F\_8I) were quasi-reversible, the second reductions were irreversible at all scan rates. This may be due to cleavage of the weak C-I bond upon adding two electrons to the compounds.

The  $\Delta E_{1/2}(0/-)$  value for 5-H-1,10-PHNZ(c-C<sub>3</sub>F<sub>6</sub>C(=O)), 0.46 V, is essentially the same as  $\Delta E_{1/2}(0/-)$  for 1,2-PHNZ(c-C<sub>4</sub>F<sub>8</sub>), 0.48 V, as shown in Fig. 14. This is significant because the former compound is a derivative of 5,10-dihydrophenazine, which would be expected to be much more difficult to reduce than analogous derivatives of PHNZ.

#### 3. Conclusions

In summary, we explored thermal and photochemical reactions of phenazine with  $C_4F_8I_2$  under a variety of experimental conditions in search of a more efficient, scalable method to prepare fluorinated

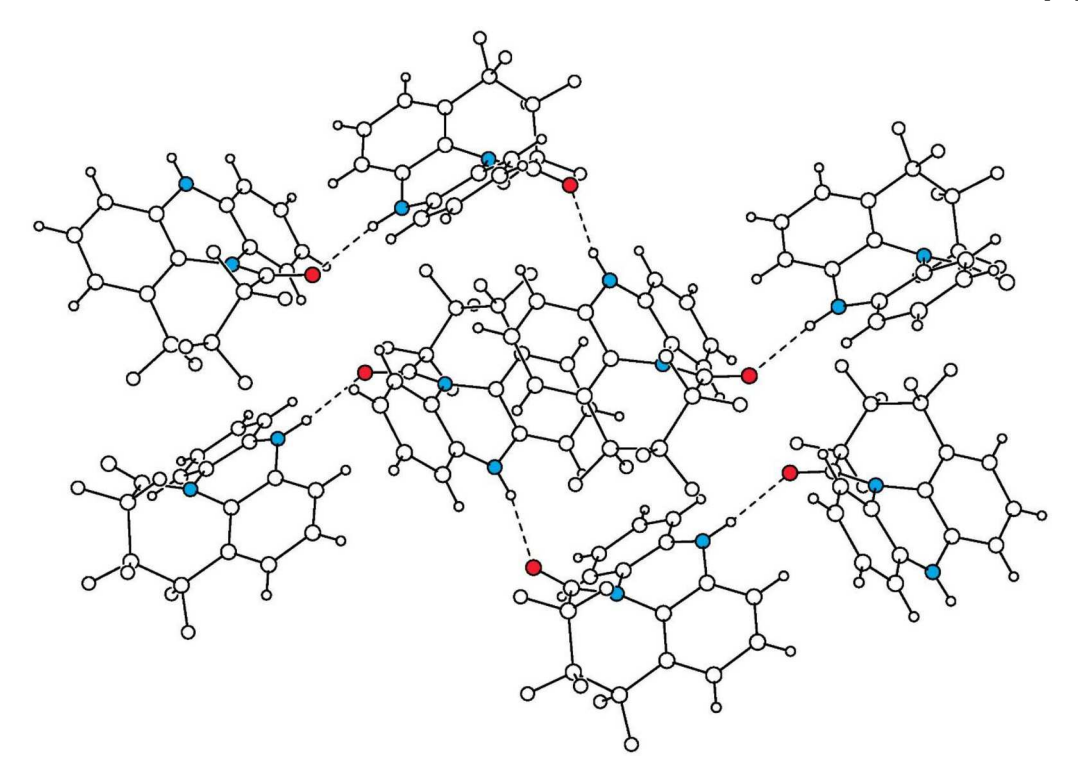


Fig. 10. The network of C=O•••H-N hydrogen bonds in the structure of 5-H-1,10-PHNZ(c-C<sub>3</sub>F<sub>6</sub>C(=O)). The O•••H, and O•••N distances and O•••H-N angle are 2.06 Å, 2.976(2) Å, and 171°, respectively, for one type of hydrogen bond and 2,08 Å, 2.957(2) Å, and 168°, respectively, for the other type of hydrogen bond.

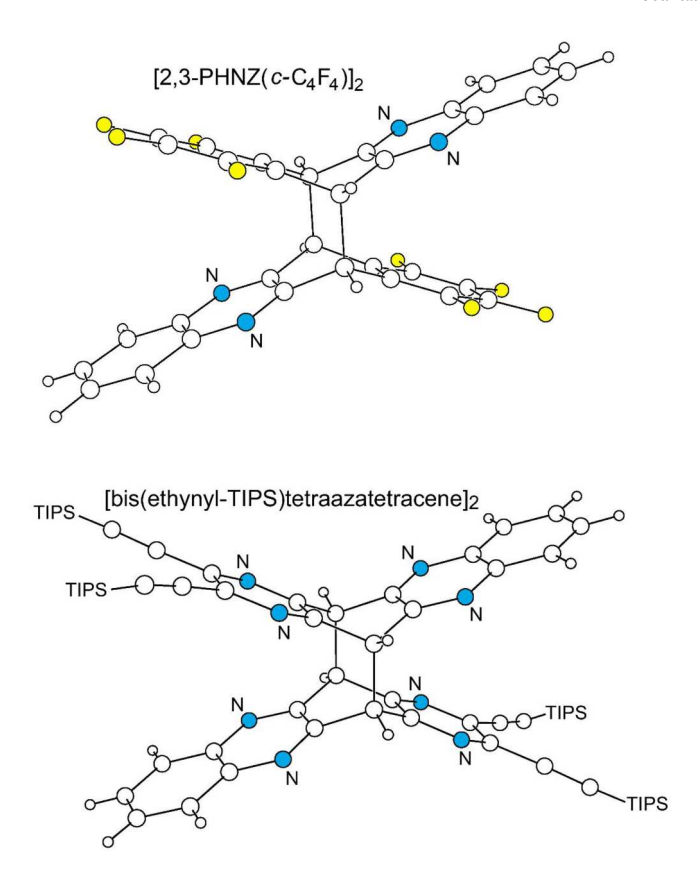


Fig. 11. Comparison of the [4+4] cycloaddition dimers  $[2,3-PHNZ(c-C_4F_4)]_2$  (top; this work) and  $[tetraazatetracene(C_C-TIPS)_2]_2$  (ref. [39].). The Si( $i-C_3H_7$ ) $_3$  groups have been abbreviated to "TIPS" for clarity.

phenazines than the methods known prior to this work [19,24]. We demonstrated that the mild photochemical methods originally developed for electron-rich arenes and monocyclic heteroarenes [44,46,82] can be successfully adjusted to phenazine, and produce not only acyclic perfluoroalkyl derivatives, but also cyclic products, when  $C_4F_8I_2$  is used as perfluoroalkylating reagent. While some reaction steps may still be desired to have greater selectivity and higher yields, the overall result exceeds the previously reported one for phenazine perfluoroalkylations

[14,24], and especially for the RDF/A for large aromatic systems, which now can be achieved selectively and nearly quantitatively. The facile synthetic techniques and purification methods developed here make these new fluorous phenazines accessible for studies as components of organic electronic devices, as valuable molecular building blocks with pronounced acceptor properties for constructing larger azaacene structures as n-type semiconductors. Extending the simple two-step approach shown in Fig. 3, it will be possible to design partially fluorinated

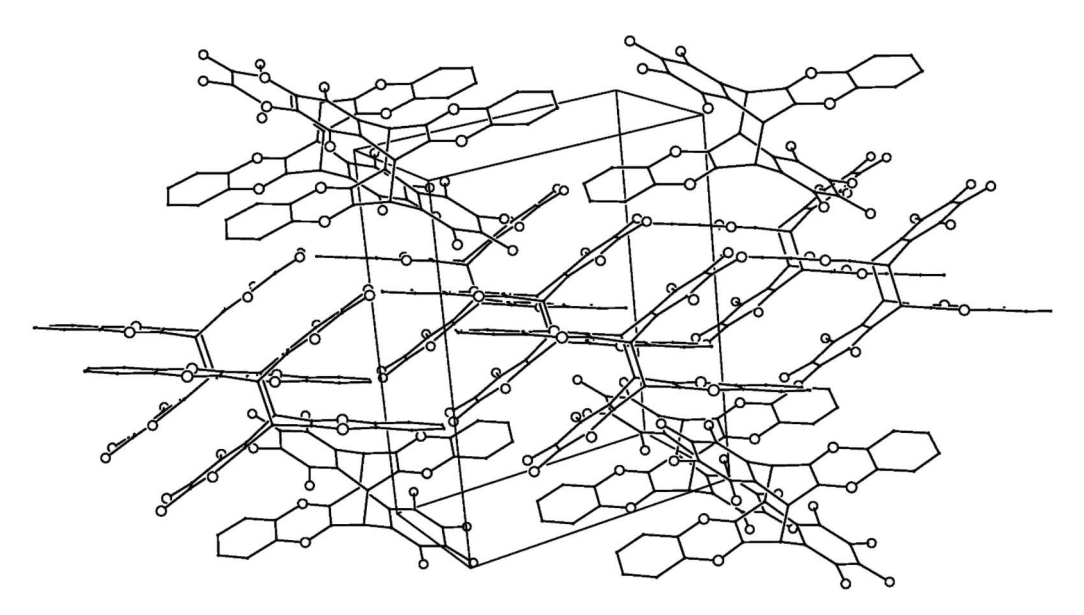


Fig. 12. The packing of molecules in the structure of  $[2,3-PHNZ(c-C_4F_4)]_2$ . The C atoms are shown as points and the H atoms have been omitted for clarity. There is no intermolecular  $\pi$ – $\pi$  overlap in this structure.

**Table 4** Electrochemical  $E_{1/2}(0/-)$  values for PHNZ, perfluoroalkylated PHNZ derivatives, and related compounds. <sup>a,b</sup>

compound	solvent/electrolyte	$E_{1/2}(0/-) / V \text{ vs. FeCp}_2^{+/0}$	$\Delta E_{1/2}(0/-) / V \text{ vs. PHNZ}^{0/-}$	$\Delta E_{1/2}(0/-) / V \text{ vs. DAZT}^{0/-}$	ref.
PHNZ	CH <sub>3</sub> CN/0.1 M TBAPF <sub>6</sub>	-1.62	0.00		
2,3-PHNZ(c-C <sub>4</sub> F <sub>4</sub> ) [7,8,9,10-DAZT(F) <sub>4</sub> ]	CH <sub>3</sub> CN/0.1 M TBAPF <sub>6</sub>	-1.36	0.26		
$1,2\text{-PHNZ}(c\text{-}C_4F_4)$	CH <sub>3</sub> CN/0.1 M TBAPF <sub>6</sub>	-1.44	0.18		
$2\text{-PHNZ}(\omega\text{-C}_4\text{F}_8\text{I})$	CH <sub>3</sub> CN/0.1 M TBAPF <sub>6</sub>	-1.29	0.33		
$1\text{-PHNZ}(\omega\text{-C}_4\text{F}_8\text{I})$	CH <sub>3</sub> CN/0.1 M TBAPF <sub>6</sub>	-1.25	0.37		
$2,3-PHNZ(c-C_4F_8)$	CH <sub>3</sub> CN/0.1 M TBAPF <sub>6</sub>	-1.04	0.58		
$1,2\text{-PHNZ}(c\text{-}C_4F_8)$	CH <sub>3</sub> CN/0.1 M TBAPF <sub>6</sub>	-1.14	0.48		
1,2,7,8-PHNZ(c-C <sub>4</sub> F <sub>8</sub> ) <sub>2</sub>	CH <sub>3</sub> CN/0.1 M TBAPF <sub>6</sub>	-0.73	0.89		[24]
1,2,6,7-PHNZ(c-C <sub>4</sub> F <sub>8</sub> ) <sub>2</sub>	CH <sub>3</sub> CN/0.1 M TBAPF <sub>6</sub>	-0.81	0.81		[24]
5-H-1,10-PHNZ( $c$ -C <sub>3</sub> F <sub>6</sub> C(=O))	CH <sub>3</sub> CN/0.1 M TBAPF <sub>6</sub>	-1.16	0.46		
PHNZ	DME/0.1 M TBAClO <sub>4</sub>	-1.74	0.00		[14]
PHNZ(CF <sub>3</sub> ) <sub>2</sub> <sup>c</sup>	DME/0.1 M TBAClO <sub>4</sub>	-1.21	0.53		[14]
1,4,6,9-PHNZ(CF <sub>3</sub> ) <sub>4</sub>	DME/0.1 M TBAClO <sub>4</sub>	-0.97	0.77		[14]
1,3,6,9-PHNZ(CF <sub>3</sub> ) <sub>4</sub>	DME/0.1 M TBAClO <sub>4</sub>	-0.92	0.82		[14]
PHNZ	DCM/0.1 M TBAPF <sub>6</sub>	-1.78	0.00		
1,2-PHNZ(c-C <sub>4</sub> F <sub>4</sub> )	DCM/0.1 M TBAPF <sub>6</sub>	-1.63	0.15		
DAZT	THF/0.1 M TBAPF <sub>6</sub>	-1.44	0.34 <sup>d</sup>	$0.00^{e}$	[66]
1,3-DAZT(F) <sub>2</sub>	DCM/0.1 M TBAPF <sub>6</sub>	-1.32	0.46	0.12 <sup>e</sup>	[24]
1,2,3,4-DAZT(F) <sub>4</sub>	DCM/0.1 M TBAPF <sub>6</sub>	-1.25	0.53	0.19 <sup>e</sup>	[24]
1,2,3,4,5,6-DAZP(F) <sub>6</sub>	DCM/0.1 M TBAPF <sub>6</sub>	-0.92			[24]

<sup>&</sup>lt;sup>a</sup>All results from this work unless otherwise indicated.

<sup>&</sup>lt;sup>b</sup>All  $E_{1/2}$  values in this table were determined by cyclic voltammetry and are  $\pm 0.01$  V. The  $\Delta E_{1/2}(0/-)$  values are relative to the PHNZ  $E_{1/2}(0/-)$  value in that solvent unless otherwise indicated. Abbreviations: PHNZ = phenazine; DAZT = 5,12-diazatetracene; DAZP = 7,14-diazapentacene; DCM = dichloromethane; DME = 1,2-dimethoxyethane; THF = tetrahydrofuran; TBAPF<sub>6</sub> = N(n-Bu)<sub>4</sub>PF<sub>6</sub>; TBAClO<sub>4</sub> = N(n-Bu)<sub>4</sub>ClO<sub>4</sub>. The dielectric constants for CH<sub>3</sub>CN, DCM, DME, and THF at 20 °C are 36.6, 9.1, 7.3, and 7.5, respectively.  $^c$  Mixture of isomers.  $^d$  Relative to the PHNZ  $E_{1/2}(0/-)$  value in DCM.  $^e$  Relative to the DAZT  $E_{1/2}(0/-)$  value in THF.

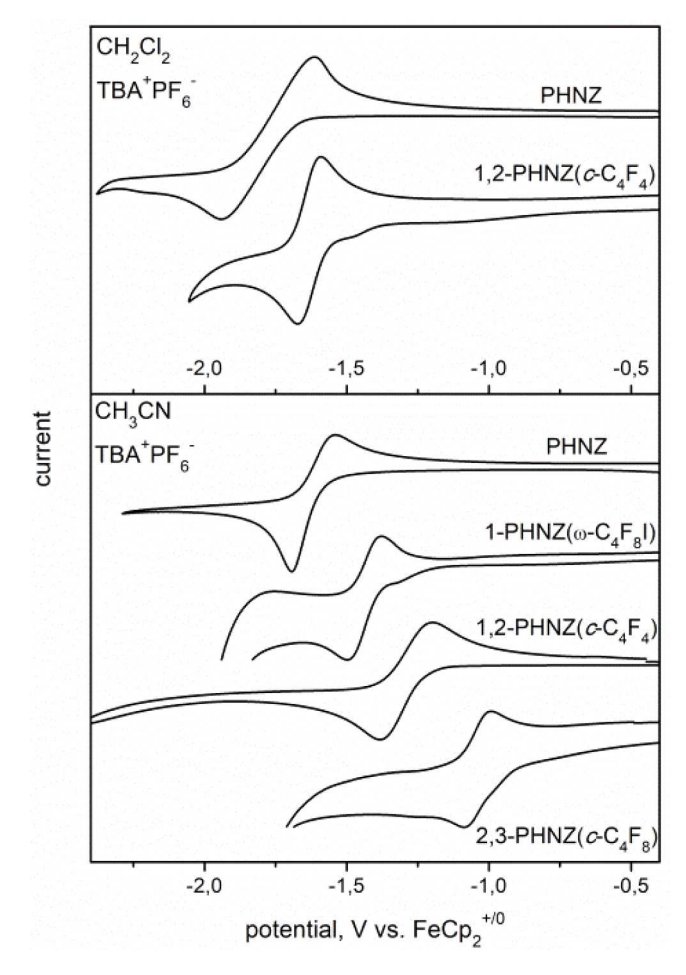


**Fig. 13.** Cyclic voltammograms of phenazine (PHNZ) and PHNZ derivatives prepared in this work. The reversible oxidation/reduction of the internal standard FeCp<sub>2</sub>, which was added to each sample after recording the shown cycles, is not shown. All cyclic voltammograms were recorded with a scan rate of 50 mV s $^{-1}$ .

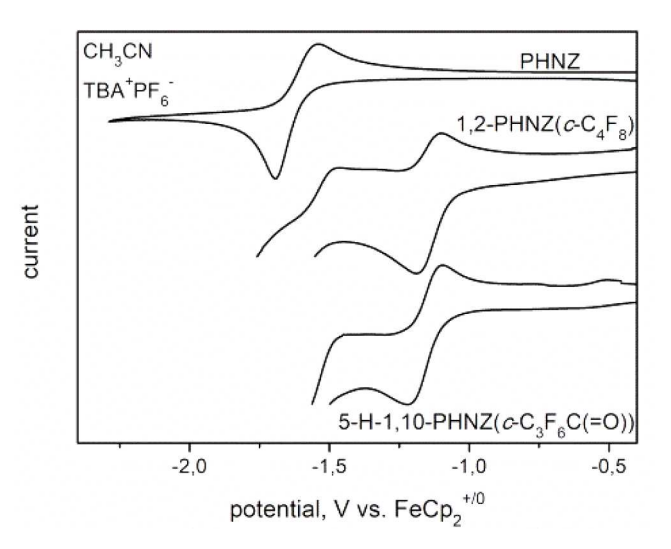


**Fig. 14.** Cyclic voltammograms of phenazine (PHNZ), 1,2-PHNZ(c-C<sub>4</sub>F<sub>8</sub>), and 5-H-1,10-PHNZ(c-C<sub>3</sub>F<sub>6</sub>C(=O)). The reversible oxidation/reduction of the internal standard FeCp<sub>2</sub>, which was added to each sample after recording the shown cycles, is not shown. All cyclic voltammograms were recorded with a scan rate of 50 mV s<sup>-1</sup>.

molecular nanographenes with varying shapes, sizes and electronic and photophysical properties tuned for a specific application. For example, bowl-shaped CORA was previously functionalized with C<sub>4</sub>F<sub>8</sub> groups forming seven- and six-member cycles, but reductive RDF/A to extend its  $\pi$ -system with partially fluorinated rings has not been attempted. The effective RDF/A with Zn dust from this work may be now applied to this and other known thermally stable PAH(C<sub>4</sub>F<sub>8</sub>)<sub>n</sub>, with PAHs such as TRPH, PHAN, ANTH [12,16,17,24]. Electrochemical studies of the PHNZ  $(\omega$ -C<sub>4</sub>F<sub>8</sub>I), PHNZ(c-C<sub>4</sub>F<sub>8</sub>), and PHNZ(c-C<sub>4</sub>F<sub>4</sub>) compounds synthesized in this work revealed large cathodic shifts relative to underivatized phenazine, including a 370 mV cathodic shift caused by substitution with a single  $\omega$ -C<sub>4</sub>F<sub>8</sub>I group, making these and similar compounds particularly attractive for organic electronics and possibly also the next generation of organic flow batteries.

#### **Declaration of Competing Interest**

None.

#### Acknowledgements

MZ is grateful to Thomas Rehm from Fraunhofer IMM (Mainz, Germany) for helping design the photo flow reactor. OVB and SHS thank the U.S. National Science Foundation (Grant CHEM-1362302) for partial support. OVB acknowledges Alexander von Humboldt Foundation for Research Grant. NSF's ChemMatCARS Sector 15 is supported by the Divisions of Chemistry (CHE) and Materials Research (DMR), National Science Foundation, under grant number NSF/CHE-1834750. Use of the Advanced Photon Source, an Office of Science User Facility operated for the U.S. Department of Energy (DOE) Office of Science by Argonne National Laboratory, was supported by the U.S. DOE under Contract No. DE-AC02-06CH11357.

#### Supplementary materials

Supplementary material associated with this article can be found, in the online version, at doi:10.1016/j.jfluchem.2022.109960.

#### References

- A. Postigo, Aromatic radical perfluoroalkylation reactions, Can. J. Chem. 90 (2012) 493–497.
- [2] T. Fujiwara, D. O'Hagan, Successful fluorine-containing herbicide agrochemicals, J. Fluorine Chem. 167 (2014) 16–29.
- [3] S. Barata-Vallejo, S.M. Bonesi, A. Postigo, Perfluoroalkylation reactions of (hetero) arenes, RSC Adv 5 (2015) 62498–62518.
- [4] H. Sun, J.H. Kramer, Perfluoroalkylated PAH n-Type Semiconductors: Theory and Experiment, in: O.V. Boltalina, T. Nakajima (Eds.), New Fluorinated Carbons: Fundamentals and Applications, Elsevier, Amsterdam, The Netherlands, 2017, pp. 155–176.
- [5] A. Postigo, Electron Donor-Acceptor Complexes in Perfluoroalkylation Reactions, Eur. J. Org. Chem. (2018) 6391–6404.
   [6] S. Barata-Vallejo, M.V. Cooke, A. Postigo, Radical Fluoroalkylation Reactions, ACS
- Catal 8 (2018) 7287–7307.

  [7] H.X. Song, Q.Y. Han, C.L. Zhao, C.P. Zhang, Fluoroalkylation reactions in aqueous
- [7] H.X. Song, Q.Y. Han, C.L. Zhao, C.P. Zhang, Fluoroalkylation reactions in aqueous media: a review, Green Chem. 20 (2018) 1662–1731.
- [8] B. Varga, B.L. Tóth, F. Béke, J.T. Csenki, A. Korschy, Z. Novák, Photochemical Application of Hydrofluoroolefin (HFO) Based Fluoroalkyl Building Block, Org. Lett. 23 (2021) 4925–4929.
- [9] W.P. Gallagher, C.A. Guerrero, F. Gonzalez-Bobes, J.R. Coombs, Radical Perfluoroalkylation of Arenes via Carbanion Intermediates, J. Org. Chem. 86 (2021) 10903–10913.
- [10] L. Helmecke, M. Apittler, B.M. Schmidt, C. Czekelius, Metal-Free Iodoperfluoroalkylation: Photocatalysis versus Frustrated Lewis Pair Catalysis, Synthesis 53 (2021) 123–134.
- [11] I.V. Kuvychko, K.P. Castro, S.H.M. Deng, X.B. Wang, S.H. Strauss, O.V. Boltalina, Taming Hot CF<sub>3</sub> Radicals: Incrementally Tuned Families of Polyarene Electron Acceptors for Air-Stable Molecular Optoelectronics, Angew. Chem. Int. Ed. 52 (2013) 4871–4874.
- [12] I.V. Kuvychko, C. Dubceac, S.H.M. Deng, X.B. Wang, A.A. Granovsky, A.A. Popov, M.A. Petrukhina, S.H. Strauss, O.V. Boltalina, C<sub>20</sub>H<sub>4</sub>(C<sub>4</sub>F<sub>8</sub>)<sub>3</sub>: A Fluorine-Containing Annulated Corannulene that Is a Better Electron Acceptor Than C<sub>60</sub>, Angew. Chem. Int. Ed. 52 (2013) 7505–7508.
- [13] I.V. Kuvychko, T. Clikeman, C. Dubceac, Y.S. Chen, M.A. Petrukhina, S.H. Strauss, A.A. Popov, O.V. Boltalina, Understanding Polyarene Trifluoromethylation with Hot CF<sub>3</sub> Radicals Using Corannulene, Eur. J. Org. Chem. (2018) 4233–4245.
- [14] K.P. Castro, T.T. Clikeman, N.J. DeWeerd, E.V. Bukovsky, K.C. Rippy, I. V. Kuvychko, G.L. Hou, Y.S. Chen, X.B. Wang, S.H. Strauss, O.V. Boltalina, Incremental Tuning Up of Fluorous Phenazine Acceptors, Chem. Eur. J. 22 (2016) 3930–3936.
- [15] T.T. Clikeman, E.V. Bukovsky, X.B. Wang, Y.S. Chen, G. Rumbles, S.H. Strauss, O. V. Boltalina, Core Perylene Diimide Designs via Direct Bay- and ortho-(Poly) trifluoromethylation: Synthesis, Isolation, X-ray Structures, Optical and Electronic Properties, Eur. J. Org. Chem. (2015) 6641–6654.
- [16] K.C. Rippy, E.V. Bukovsky, T.T. Clikeman, Y.S. Chen, G.L. Hou, X.B. Wang, A. A. Popov, O.V. Boltalina, S.H. Strauss, Copper Causes Regiospecific Formation of C4F<sub>8</sub>-Containing Six-Membered Rings and their Defluorination/Aromatization to C4F<sub>4</sub>-Containing Rings in Triphenylene/1,4-C<sub>4</sub>F<sub>8</sub>I<sub>2</sub> Reactions, Chem. Eur. J. 22 (2016) 874–877.
- [17] K.C. Rippy, N.J. DeWeerd, I.V. Kuvychko, Y.S. Chen, S.H. Strauss, O.V. Boltalina, Fluorination-Induced Evolution of Columnar Packing in Fluorous Triphenylenes and Benzotriphenylenes, ChemPlusChem 83 (2018) 1067–1077.

- [18] L.K. San, T.T. Clikeman, C. Dubceac, A.A. Popov, Y.S. Chen, M.A. Petrukhina, S. H. Strauss, O.V. Boltalina, Corannulene Molecular Rotor with Flexible Perfluorobenzyl Blades: Synthesis, Structure and Properties, Chem. Eur. J. 21 (2015) 9488–9492.
- [19] L.K. San, E.V. Bukovsky, I.V. Kuvychko, A.A. Popov, S.H. Strauss, O.V. Boltalina, Single-step gas-phase polyperfluoroalkylation of naphthalene leads to thermodynamic products, Chem. Eur. J. 20 (2014) 4373–4379.
- [20] B. Almeddine, O.F. Aebischer, W. Amrein, B. Donnio, R. Deschenaux, D. Guillon, C. Savary, D. Scanu, O. Scheidegger, T.A. Jenny, Mesomorphic Hexabenzocoronenes Bearing Perfluorinated Chains, Chem. Mater. 17 (2005) 4798–4807.
- [21] A.G. Hudson, M.L. Jenkins, A.E. Pedler, J.C. Tatlow, The Electrochemical Oxidation of Polyfluoroaromatic Amines. II. The Synthesis of Substituted Polyfluorophenazines, Tetrahedron 26 (1970) 5781–5787.
- [22] T.I. Filyakova, V.I. Filyakova, A.Y. Zapevalov, M.I. Kodess, P.A. Slepukhin, V. I. Saloutin, V.N. Charushin, New derivatives of fluorine-containing phenazines, Mendeleev Commun. 37 (2017) 290–292.
- [23] M.M. Khusniyarov, K. Harms, J. Sundermeyer, New highly fluorinated phenazine derivatives: Correlation between crystal structure and NMR spectroscopy, J. Fluorine Chem. 127 (2006) 200–204.
- [24] K.C. Rippy, Synthesis and Evaluation of Fluorous Polycyclic Aromatic Hydrocarbon Derivatives for Organic Electronics, Ph.D. Dissertation, Colorado State University (2019).
- [25] J. Schwaben, N. Münster, M. Klues, T. Breuer, P. Hofmann, K. Harms, G. Witte, U. Koert, Efficient Syntheses of Novel Fluoro-Substituted Pentacenes and Azapentacenes: Molecular and Solid-State Properties, Chem. Eur. J. 21 (2015) 13758–13771.
- [26] J.U. Engelhart, B.D. Lindner, O. Tverskoy, F. Rominger, U.H.F. Bunz, Partially Fluorinated Tetraazaacenes by Nucleophilic Aromatic Substitution, J. Org. Chem. 78 (2013) 10832–10839.
- [27] S. Yamada, K. Kinoshita, S. Iwama, T. Yamazaki, T. Kubota, T. Yajima, K. Yamamoto, S. Tahara, Synthesis of perfluoroalkylated pentacenes and evaluation of their fundamental physical properties, Org. Biomol. Chem. 15 (2017) 2522–2535.
- [28] H. Sun, U.K. Tottempudi, J.D. Mottishaw, P.N. Basa, A. Putta, A.G. Sykes, Strengthening π-π Interactions While Suppressing C<sub>sp2</sub>-H•••π (T-Shaped) Interactions via Perfluoroalkylation: A Crystallographic and Computational Study That Supports the Beneficial Formation of 1-D π-π Stacked Aromatic Materials, Cryst. Growth Des. 12 (2012) 5655-5662.
- [29] A. Putta, J.D. Mottishaw, Z. Wang, H. Sun, Rational Design of Lamellar π–π Stacked Organic Crystalline Materials with Short Interplanar Distance, Cryst. Growth Des. 14 (2014) 350–356.
- [30] H.P. Cao, J.C. Xiao, Q.Y. Chen, Fluoroalkylation of aromatics: An intramolecular radical cyclization of 4-chloro-1,1,2,2,3,3,4,4-octafluorobutylbenzenes, J. Fluorine Chem. 127 (2006) 1079–1086.
- [31] P.T. Kaplan, L. Xu, B. Chen, K.R. McGarry, S. Yu, H. Wang, D.A. Vicic, Mild, Safe, and Versatile Reagents for (CF<sub>2</sub>)n Transfer and the Construction of Fluoroalkyl-Containing Rings, Organometallics 32 (2013) 7552–7558.
- [32] P.T. Kaplan, B. Chen, D.A. Vicic, Synthetic utility of dizinc reagents derived from 1,4-diiodo- and 1,4-dibromooctafluorobutane, J. Fluorine Chem. 168 (2015) 158–162.
- [33] P.T. Kaplan, D.A. Vicic, Versatile Route to Arylated Fluoroalkyl Bromide Building Blocks, Org. Lett. 18 (2016) 864–886.
- [34] Y. Li, C. Li, W. Yue, W. Jiang, R. Kopecek, J. Qu, Z. Wang, Direct functionalization of polycyclic aromatics via radical perfluoroalkylation, Org. Lett. 12 (2010) 2374–2377
- [35] I. Pibiri, S. Buscemi, A.P. Piccionello, M.L. Saladino, D.C. Martino, E. Caponetti, Photochemical synthesis of pyrene perfluoroalkyl derivatives and their embedding in a polymethylmethacrylate matrix: a spectroscopic and structural study, J. Mater. Chem. C 2 (2014) 7722–7730.
- [36] M. Iizuka, M. Yoshida, Redox system for perfluoroalkylation of arenes and α-methylstyrene derivatives using titanium oxide as photocatalyst, J. Fluorine Chem. 130 (2009) 926–932.
- [37] L. Cui, T. Ono, M.J. Hossain, Y. Hisaeda, Electrochemically driven, cobalt–carbon bond-mediated direct intramolecular cyclic and acyclic perfluoroalkylation of (hetero) arenes using X(CF<sub>2</sub>)<sub>4</sub>X, RSC Adv 10 (2020) 24862–24866.
- [38] L.M. Jin, L. Chen, C.C. Guo, Q.Y. Chen, Copper-induced fluoroalkylation of porphyrins: solvent-dependent synthesis of fluoroalkyl chlorins and porphyrins from fluoroalkyl iodides, J. Porphyr. Phthacyanines 9 (2005) 109–120.
- [39] T. Agou, S. Suzuki, Y. Kanno, T. Hosoya, H. Fukumoto, Y. Mizuhata, N. Tokitoh, Y. Suda, S. Furukawa, M. Saito, T. Kubota, Synthesis and properties of perfluoroalkylated TIPS-pentacenes, Tetrahedron 75 (2019), 130678.
- [40] A. Bravo, H.R. Bjørsvik, F. Fontana, L. Liguori, A. Mele, F. Minisci, New methods of free-radical perfluoroalkylation of aromatics and alkenes. Absolute rate constants and partial rate factors for the homolytic aromatic substitution by n-perfluorobutyl radical, J. Org. Chem. 62 (1997) 7128–7136.
- [41] O.A. Tomashenko, V.V. Grushin, Aromatic trifluoromethylation with metal complexes, Chem. Rev. 111 (2011) 4475–4521.
- [42] M. Salamone, L. Mangiacapra, M. Bietti, Kinetic Solvent Effects on the Reactions of the Cumyloxyl Radical with Tertiary Amides. Control over the Hydrogen Atom Transfer Reactivity and Selectivity through Solvent Polarity and Hydrogen Bonding, J. Org. Chem. 80 (2015) 1149–1154.
- [43] S. Samai, S. Rouichi, A. Ferhati, A. Chakir, N,N-dimethylformamide (DMF), and N, N-dimethylacetamide (DMA) reactions with NO<sub>3</sub>, OH and Cl: A theoretical study of the kinetics and mechanisms, Arab. J. Chem. 12 (2019) 4957–4970.

- [44] S. Barata-Vallejo, S.M. Bonesi, A. Postigo, Photocatalytic fluoroalkylation reactions of organic compounds, Org. Biomol. Chem. 13 (2015) 11153–11183.
- [45] Y. Wang, J. Wang, G.X. Li, G. He, G. Chen, Halogen-bond-promoted photoactivation of perfluoroalkyl iodides: A photochemical protocol for perfluoroalkylation reactions, Org. Lett. 19 (2017) 1442–1445.
- [46] S. Barata-Vallejo, M.M. Flesia, B. Lantaño, J.E. Argüello, A.B. Peñéñory, A. Postigo, Heterogeneous Photoinduced Homolytic Aromatic Substitution of Electron-Rich Arenes with Perfluoroalkyl Groups in Water and Aqueous Media–A Radical-Ion Reaction, Eur. J. Org. Chem. (2013) 998–1008.
- [47] C. Rosso, J.D. Williams, G. Filippini, M. Prato, C.O. Kappe, Visible-light-mediated iodoperfluoroalkylation of alkenes in flow and its application to the synthesis of a key fulvestrant intermediate, Org. Lett. 21 (2019) 5341–5345.
- [48] S. Barata-Vallejo, D.E. Yerien, A. Postigo, Benign Perfluoroalkylation of Aniline Derivatives through Photoredox Organocatalysis under Visible-Light Irradiation, Eur. J. Org. Chem. (2015) 7869–7875.
- [49] S.M. Linden, D.C. Neckers, Fundamental properties of Rose Bengal. 25. Bleaching studies of Rose Bengal onium salts, J. Am. Chem. Soc. 110 (1988) 1257–1260.
- [50] T.H. Rehm, Reactor technology concepts for flow photochemistry, ChemPhotoChem 4 (2020) 235–254.
- [51] J.D. Williams, C.O. Kappe, Recent advances toward sustainable flow photochemistry, Curr. Opin. Green Sustain. Chem. 25 (2020), 100351.
- [52] N.J. Straathof, H.P. Gemoets, X. Wang, J.C. Schouten, V. Hessel, T. Noël, Rapid trifluoromethylation and perfluoroalkylation of five-membered heterocycles by photoredox catalysis in continuous flow, ChemSusChem 7 (2014) 1612–1617.
- [53] Y. Sakamoto, T. Suzuki, M. Kobayashi, Y. Gao, Y. Fukai, Y. Inoue, F. Sato, S. Tokito, Perfluoropentacene: High-Performance p—n junctions and complementary circuits with pentacene, J. Am. Chem. Soc. 126 (2004) 8138–8140.
- [54] L. Chen, L.M. Jin, C.C. Guo, Q.Y. Chen, Fluoroalkylation of porphyrins: Generation of 2-and 20-perfluoroalkyl-5,10,15-triarylporphyrin radicals and their intramolecular cyclizations, Synlett (2005) 0963–0970.
- [55] D. Bischof, M. Zeplichal, S. Anhäuser, A. Kumar, M. Kind, F. Kramer, M. Bolte, S. I. Ivlev, A. Terfort, G. Witte, Perfluorinated Acenes: Crystalline Phases, Polymorph-Selective Growth, and Optoelectronic Properties, J. Phys. Chem. C 125 (2021) 19000–19012.
- [56] K.P. Castro, E.V. Bukovsky, I.V. Kuvychko, N.J. DeWeerd, Y.S. Chen, S.H.M. Deng, X.B. Wang, A.A. Popov, S.H. Strauss, O.V. Boltalina, PAH/PAH(CF<sub>3</sub>)<sub>n</sub> Donor/ Acceptor Charge-Transfer Complexes in Solution and in Solid-State Co-Crystals, Chem. Eur. J. 25 (2019) 1354–13565.
- [57] D.D.L. Chung, Graphite, J. Mater. Sci. 37 (2002) 1475-1489.
- [58] T. Dahl, The Nature of Stacking Interactions between Organic Molecules Elucidated by Analysis of Crystal Structures, Acta Chem. Scand. 48 (1994) 95–106.
- [59] K. Woźniak, B. Kariuki, W. Jones, Structure of Phenazine, Acta Crystallogr., Sect. C, Struct. Chem. 47 (1991) 1113–1114.
- [60] W. Jankowski, M. Gdaniec, The β-polymorph of phenazine, Acta Crystallogr., Sect. C. Cryst. Struct. Commun. 58 (2002) 0181–0182.
- [61] A. Bondi, van der Waals Volumes and Radii, J. Phys. Chem. 68 (1964) 441-451.
- [62] E. Corradi, S.V. Meille, M.T. Messina, P. Metrangolo, G. Resnati, Perfluorocarbonhydrocarbon self-assembly. Part 6: α,ω-Diiodoperfluoroalkanes as pseudohalogens in supramolecular synthesis, Tetrahedron Lett 40 (1999) 7519–7523.
  [63] G. Cavallo, P. Metragolo, R. Milani, T. Pilati, A. Priimagi, G. Resnati, G. Terraneo,
- [63] G. Cavallo, P. Metragolo, R. Milani, T. Pilati, A. Priimagi, G. Resnati, G. Terraneo The Halogen Bond, Chem. Rev. 116 (2016) 2478–2601.
- [64] V.R. Thalladi, T. Smolka, A. Gehrke, R. Boese, R. Sustmann, Role of weak hydrogen bonds in the crystal structures of phenazine, 5,10-dihydrophenazine and their 1:1 and 3:1 molecular complexes, New J. Chem. 24 (2000) 143–147.

- [65] P. Reboul, Y. Oddon, C. Caranoni, J.C. Soyfer, J. Barbe, G. Pèpe, Structure du Dihydro-9,10 Anthracène. Support Tricyclique de Médicaments Psychotropes, Acta Crystallogr., Sect. C, Struct. Chem. 43 (1987) 537–539.
- [66] M. Märken, B.D. Lindner, A.L. Appleton, F. Rominger, U.H.F. Bunz, Synthesis of tetraazatetracenes and -pentacenes: role of the substituents for their stability, Pure Appl. Chem. 86 (2014) 483–488.
- [67] N. Ando, M. Mitsui, Comprehensive photoelectron spectroscopic study of anionic clusters of anthracene and its alkyl derivatives: Electronic structures bridging molecules to bulk, J. Chem. Phys. 127 (2007), 234305.
- [68] G.W. Dillow, P. Kebarle, Electron affinities of aza-substituted polycyclic aromatic hydrocarbons, Can. J. Chem. 67 (1989) 1628–1631.
- [69] T. Kubota, K. Kano, B. Uno, T. Konse, Energetics of the Sequential Electroreduction and Electrooxidation Steps of Benzenoid Hydrocarbons, Bull. Chem. Soc. Jpn. 60 (1987) 3865–3877.
- [70] A.P. Davis, A.J. Fry, Experimental and Computed Absolute Redox Potentials of Polycyclic Aromatic Hydrocarbons are Highly Linearly Correlated Over a Wide Range of Structures and Potentials, J. Phys. Chem. A 114 (2010) 12299–12304.
- [71] S. Miao, S.M. Brombosz, P.v.R. Schleyer, J.I. Wu, S. Barlow, S.R. Marder, K. I. Hardcastle, U.H.F. Bunz, Are N,N-Dihydrodiazatetracene Derivatives Antiaromatic? J. Am. Chem. Soc. 130 (2008) 7339–7344.
- [72] N.G. Tsierkezos, Investigation of the Electrochemical Reduction of Benzophenone in Aprotic Solvents Using the Method of Cyclic Voltammetry, J. Solution Chem. 36 (2007) 1301–1310.
- [73] H. Svith, H. Jensen, J. Almstedt, P. Andersson, T. Lundbäck, K. Daasbjerg, M. Jonsson, On the Nature of Solvent Effects on Redox Properties, J. Phys. Chem. A 108 (2004) 4805–4811.
- [74] F.S.T. Khan, A.L. Waldbusser, M.C. Carrasco, H. Pourhadi, S. Hernatian, Synthetic, spectroscopic, structural, and electrochemical investigations of ferricenium derivatives with weakly coordinating anions: ion pairing, substituent, and solvent effects, Dalton Trans 50 (2021) 7433–7455.
- [75] C. de la Cruz, A. Molina, N. Patil, E. Ventosa, R. Marcilla, A. Mavrandonakis, New insights into phenazine-based organic redox flow batteries by using highthroughput DFT modelling, Sustain. Energy Fuels 4 (2020) 5513–5521.
- [76] D. Pache, R. Schmid, Molecular Dynamics Investigation of the Dielectric Decrement of Ion Solutions, ChemElectroChem 5 (2018) 1444–1450, and references therein.
- [77] T. Le, N.T. Tran, The Nonlinear Decrement in Static Permittivity of Electrolytes in High-Polarity Solvents, J. Solution Chem. 50 (2021) 105–115, and references therein.
- [78] L.K. San, S.N. Spisak, C. Dubceac, S.H.M. Deng, I.V. Kuvychko, M.A. Petrukhina, X. B. Wang, A.A. Popov, S.H. Strauss, O.V. Boltalina, Experimental and DFT Studies of the Electron-Withdrawing Ability of Perfluoroalkyl (R<sub>F</sub>) Groups: Electron Affinities of PAH(R<sub>F</sub>)<sub>n</sub> Increase Significantly with Increasing R<sub>F</sub> Chain Length, Chem. Eur. J. 24 (2018) 1441–1447.
- [79] M. Mitsui, N. Ando, A. Nakajima, Mass Spectrometry and Photoelectron Spectroscopy of Tetracene Cluster Anions, (Tetracene)n<sup>-</sup> (n=1-100): Evidence for the Highly Localized Nature of Polarization in a Cluster Analogue of Oligocene Crystals, J. Phys. Chem. A 111 (2007) 9644–9648.
- [80] G.D. Chen, R.G. Cooks, Electron affinities of polycyclic aromatic hydrocarbons determined by the kinetic method. J. Mass Spectrom. 30 (1995) 1167–1173.
- [81] A. Sosorev, D. Dominskiy, I. Chernyshov, R. Efremov, Tuning of Molecular Electrostatic Potential Enables Efficient Charge Transport in Crystalline Azaacenes: A Computational Study, Intl. J. Mol. Sci. 21 (2020) 5654.
- [82] S. Barata-Vallejo, D.E Yerien, B. Lantano, A. Postigo, Transition Metal-free Photoorganocatalytic Fluoroalkylation Reactions of Organic Compounds, Curr. Org. Chem. 20 (2016) 2838–2847.